



NAM

Investigation of gas presence in the aquifer of the Groningen field

Gulfiia Ishmukhametova

NAM

Datum 13 September-2017 (main report) and
September-2018 (addendum)

Editors Jan van Elk & Dirk Doornhof

General Introduction

The subsurface model of the Groningen field is used to model the first step in the causal chain from gas production to induced earthquake risk. It models the pressure response in the gas and water bearing reservoir formations to the gas extraction.

The reservoir model of the Groningen field was built in 2011 and 2012 and has a very detailed description of the faults in the field to support studies into induced earthquakes. The model was used to support Winningsplan 2013 (Ref. 1 to 3) and has since then been continuously improved (Ref. 4, 6 and 7). This report describes the continuous improvement of the subsurface model of the Groningen field and in particular the effort to update and improve the history match.

Pressure decline in the field is an important driver for compaction and therefore subsidence. Compaction in turn affects stress and strain and is therefore of importance for the mechanism inducing earthquakes. The model therefore has an important role in the optimization of the gas withdrawal from the reservoir to reduce seismicity.

For Winningsplan 2013 and Winningsplan 2016, the model was reviewed by the independent consultant SGS Horizon. An extensive assurance review (Ref. 5) with opinion letter has been prepared by SGS Horizon.

A further improvement of the dynamic reservoir model was planned in 2018. Previous updates had focussed on the forecasting of reservoir pressure in the seismically active area in the north and central area of the field. Aim of these updates was to improve seismic forecasts. The current update of the reservoir model aims at also improving the understanding of the response of the aquifers connected to the field. The presence of gas at low saturations in the aquifer of the Slochteren formation below the initial (pre-production) gas-water-contact (GWC) is important for the inflow of water from the aquifer into the depleted reservoir. The current report describes the effort to obtain observational data of gas below the GWC from logs taken in wells which expose the aquifer immediately below the GWC. New loggings tools developed by Schlumberger (PNX™ tool) were used to obtain gas saturation logs in UH-1 well. As the rock mineralogy plays an important role in the interpretation of these logs it was recommended to also run this log in ZRP-3, where based on the core taken in this well a detailed mineralogical description is available. The follow-up study based on ZRP-3 is included in this document as an addendum.

References

1. Winningsplan Groningen 2013, Nederlandse Aardolie Maatschappij BV, 29th November 2013.
2. Technical Addendum to the Winningsplan Groningen 2013; Subsidence, Induced Earthquakes and Seismic Hazard Analysis in the Groningen Field, Nederlandse Aardolie Maatschappij BV (Jan van Elk and Dirk Doornhof, eds), November 2013.
3. Supplementary Information to the Technical Addendum of the Winningsplan 2013, Nederlandse Aardolie Maatschappij BV (Jan van Elk and Dirk Doornhof, eds), December 2013.
4. Groningen Field Review 2015 Subsurface Dynamic Modelling Report, Burkitov, Ulan, Van Oeveren, Henk, Valvatne, Per, May 2016.
5. Independent Review of Groningen Subsurface Modelling Update for Winningsplan 2016, SGS Horizon, July 2016.
6. Groningen Dynamic Model Update 2018, NAM, Henk van Oeveren, Per Valvatne and Leendert Geurtsen, September 2017
7. Groningen Dynamic Model Update 2019, Quint de Zeeuw and Leendert Geurtsen, NAM, October 2018



NAM

Title	Investigation of gas presence in the aquifer of the Groningen field	Date	13 September-2017 (main report) and September-2018
		Initiator	NAM
Autor(s)	Gulfiia Ishmukhametova	Editors	Jan van Elk Dirk Doornhof
Organisation	NAM	Organisation	NAM
Place in the Study and Data Acquisition Plan	<p><u>Study Theme: Prediction Reservoir Pressure based on gas withdrawal</u></p> <p><u>Comment:</u></p> <p>The subsurface model of the Groningen field is used to model the first step in the causal chain from gas production to induced earthquake risk. It models the pressure response in the gas and water bearing reservoir formations to the gas extraction.</p> <p>The reservoir model of the Groningen field was built in 2011 and 2012 and has a very detailed description of the faults in the field to support studies into induced earthquakes. The model was used to support Winningsplan 2013 and has since then been continuously improved. This report describes the continuous improvement of the subsurface model of the Groningen field and in particular the effort to update and improve the history match.</p> <p>Pressure decline in the field is an important driver for compaction and therefore subsidence. Compaction in turn affects stress and strain and is therefore of importance for the mechanism inducing earthquakes. The model therefore has an important role in the optimization of the gas withdrawal from the reservoir to reduce seismicity.</p> <p>For Winningsplan 2013 and Winningsplan 2016, the model was reviewed by the independent consultant SGS Horizon. An extensive assurance review with opinion letter has been prepared by SGS Horizon.</p> <p>A further improvement of the dynamic reservoir model was planned in 2018. Previous updates had focussed on the forecasting of reservoir pressure in the seismically active area in the north and central area of the field. Aim of these updates was to improve seismic forecasts. The current update of the reservoir model aims at also improving the understanding of the response of the aquifers connected to the field. The presence of gas at low saturations in the aquifer of the Slochteren formation below the initial (pre-production) gas-water-contact (GWC) is important for the inflow of water from the aquifer into the depleted reservoir. The current report describes the effort to obtain observational data of gas below the GWC from logs taken in wells which expose the aquifer immediately below the GWC. New loggings tools developed by Schlumberger</p>		

	(PNX™ tool) were used to obtain gas saturation logs in UH-1 well. As the rock mineralogy plays an important role in the interpretation of these logs it was recommended to also run this log in ZRP-3, where based on the core taken in this well a detailed mineralogical description is available. The follow-up study based on ZRP-3 is included in this document as an addendum.
Directly linked research	<ul style="list-style-type: none"> • Reservoir Compaction • Optimisation of the aerial distribution of production
Used data	Sub-surface data from the Groningen field; open-hole logs, core data, pressure data, production data etc.
Associated organisation	
Assurance	



NAM

Nederlandse Aardolie Maatschappij B.V.

Shell UPO

Investigation of gas presence in the aquifer of the Groningen field

Date: 13-September-2017 (main Report) and
28th September 2018 (Addendum)

Gulfiia Ishmukhametova,

Petrophysicist

Executive Summary

A petrophysical study was initiated to investigate the presence of gas in the aquifer of the Groningen field. The initial objective of the study was straight forward: to establish gas saturations below the gas water contact based on the available open-hole log data (mainly from 1960-1980). However, the study revealed, that gas saturation below the GWC is in the range of 0-30%, which is within the uncertainties of the gas saturation assessment. The high uncertainties in the assessment of gas saturation are caused by the fact, that parameters for the water leg were assessed approximately in the previous petrophysical study. In addition it emerged, that gas saturation is highly sensitive to the rock composition. The recent geological study demonstrated that Rotliegend formation has a complex mineralogical composition. The available open-hole log data was not allowing to build petrophysical model, which can account for different minerals. The large uncertainties in saturation parameters in combination with the complex rock composition resulted in a relatively high uncertainty in the estimated gas saturation.

The recent development in cased hole reservoir surveillance technology (PNX™) enabled an opportunity for a more accurate quantification of gas saturation. The PNX™ tool provides a novel type of measurement, which is sensitive to gas and not to fluid, that can be interpreted to derive at an actual saturation value.

In April 2017 PNX™ logging was carried out on UHZ-1. The data conclusively demonstrated the presence of gas in the aquifer and results can be summarised as follows.

- A small quantity of gas was calculated in the interval below the GWC (GWC at 2969 m AHORT)
- A fairly consistent gas signature was observed down to 46 m below the GWC (over the interval from 2969 m AHORT till 3015 m AHORT) with average gas saturation value of around 8-10% with some peaks up to 20%.
- The calculated gas saturation distribution is rather patchy, i.e. discontinuous.

The acquisition of PNX™ data also helped to improve the mineralogical model of the Rotliegend formation for the well. This allowed for a reassessment of the gas saturation based on the historic open-hole log data. However, the gas saturation interpretation results based on cased hole and open-hole log data differs.

The difference between cased hole and open hole saturation interpretation may result from various causes:

- The different methodologies for assessment of saturation both carry their own uncertainty ranges. These ranges need to be further studied.
- Impact of clay mineral composition on saturation parameter determination
 - It is known that the mineral composition has an impact on the gas saturation calculation, this is true for both open and cased hole calculations. The workflows described in this document already takes this into account with the available data, however, further study would be required to improve the understanding of the clay minerals and their contribution to the saturation calculation specifically below the gas-water contact. This can be achieved by a detailed calibration of PNX™ tool responses (elemental dry weights) to the core data and a detailed review of the saturation parameters used in the open-hole calculation below the gas-water contact. It is expected that this will help to reduce the difference in the interpreted saturation values between the cased hole and open hole logs.
- Impact of depletion
 - The Open Hole logs of UHZ-1 were acquired in 1978, by which time some 650Bcm of gas was produced. As an average over the field, this equates to roughly 22% depletion with respect to initial pressure. It is possible that depletion of the aquifer has impacted the gas saturations below the gas water contact.

Once the difference is resolved, it is recommended to establish whether a representative model can be applied across the full field. If so, reinterpretation of the open-hole logs for all wells with a logging coverage over the aquifer may be required. In case gas below the aquifer is observed consistently across the field, a saturation model for gas in the

aquifer of the Groningen field should be constructed. To allow for extrapolation beyond the areas that have well coverage, this model build should be integrated with a geological/basin modelling explanation of the observations.

Table of Contents

Executive Summary	3
1 Introduction	7
2 Cased hole saturation evaluation	9
2.1 Pulsed Neutron Logging	9
2.2 New developments in logging – Pulsed Neutron Extreme.....	9
2.3 PNX™ data acquisition and processing workflow	10
3 Quantitative saturation assessment	12
3.1 General method	12
3.2 Multiminerall petrophysical analysis for complex cases.....	12
4 Estimation of the mineralogy composition.....	13
4.1 Introduction.....	13
4.2 Sand components.....	14
4.3 Clay components.....	14
5 Uithuizen-1 FNXS analysis	17
6 Multi-Mineral Petrophysical Analysis for cased hole evaluation	19
6.1 Parameter initialization	19
6.2 Main model setup.....	19
6.3 Formation components.....	21
6.4 Constraints and Constants.....	22
6.5 MMPA main outputs.....	23
6.6 MMPA cased hole results.....	25
7 Multi-Mineral Petrophysical Analysis for open hole evaluation	26
7.1 Parameter Initialization	26
7.2 Main model inputs	26
7.3 Formation components.....	27
7.4 Wet Clay Model	27
7.5 Saturation Model.....	28
7.5.1 Waxman-Smits saturation method.....	28
7.5.2 Waxman-Smits saturation parameters inputs	29
7.6 Constraints and Constants.....	30
7.7 MMPA main outputs.....	30
7.8 MMPA open hole results.....	32
8 Generalization and delimitations	32
9 Conclusions and recommendations	33
10 References	35
Investigation of gas presence in the aquifer of the Groningen field	5

Appendix 1 – FNXS new measurement (courtesy of Schlumberger)	36
Appendix 2 – Theoretical values for typical formation component (courtesy of Schlumberger)	37
Appendix 3 – List of main inputs and outputs of initialization method (Techlog™ helpfile)	38
A3.1 Inputs	38
A3.2 Outputs.....	38

1 Introduction

Over the past years, NAM has executed an extensive study programme to increase the understanding of production induced seismicity in the Groningen field (Van Elk, 2016). A specific study theme concerns with the presence of residual gas below the gas water contact was conducted. The presence of gas in the aquifer might play an important role in the dynamic behaviour of the Groningen field (Van Oeveren, 2015). There are various indications of gas below the contact, including direct measurements:

- Calculated gas saturation from open-hole logs (although the measurement uncertainty is high within the water leg).

There are also indirect measurements that suggest the presence of gas below the contact:

- Based on synthetic seismic created from the Groningen static model a sharp transition between a gas-saturated and a gas-free zone is expected to show up as a clear direct hydrocarbon indicator. However, this is not observed in the actual seismic, suggesting that the underlying aquifer does contain certain amounts of residual gas.
- Repeat formation tests (RFT) indicate a significant pressure lag between the pores below the gas water contact, with respect to the gas saturated pores above the contact. This could imply gas saturation, which significantly slows depletion due to a relative permeability effect and a compressibility effect (van Oeveren,2015). The effect of gas in the aquifer might significantly impact the pressure behaviour in the water leg, the aquifer influx and the pressure support to the main field. When gas saturation is introduced below the contact in a dynamic model, the model response seems to better capture this pressure lag, this is shown for Uiterhuizen-1 in Figure. 1.

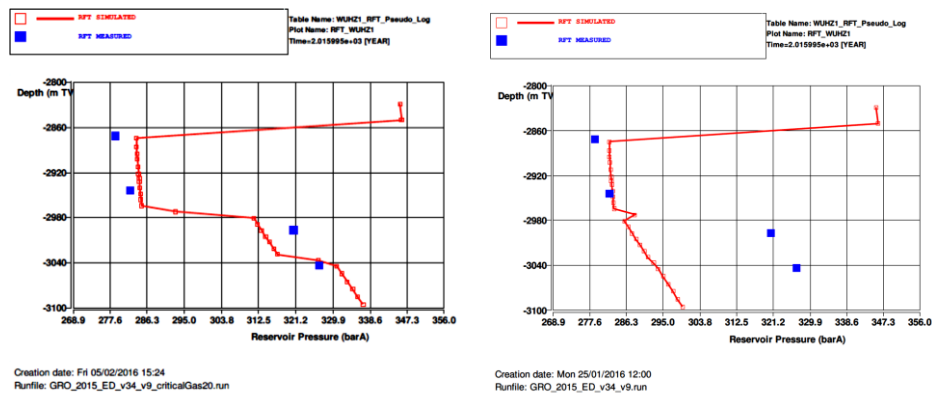


Figure 1: RFT data (blue squares) compared to model output (red line), to the left -model initialized with gas in the aquifer, to the right- without gas (van Oeveren,2015)

A petrophysical study was initiated to investigate the presence of gas in the aquifer of the Groningen field. The initial outset of the study was relatively simple: to establish gas saturations below the gas water contact based on the available open hole log data. A cased hole log was added to the scope which applied the newly available PNX technology. The results from this log increased the scope of the study, which ultimately addressed the following objectives:

- Validate the presence of gas in the aquifer through dedicated data acquisition (PNX™)
- Validate the presence of gas in the aquifer through integrated re-interpretation of existing data from open-hole logs

- Provide a quantitative assessment of gas saturation for the interval below the gas water contact (best assessment for the given measurement uncertainties)

Water saturation determination (S_w) is one of the most challenging of petrophysical calculations and is used to quantify the hydrocarbon (gas) saturation ($1 - S_w$) (Petrowiki.org). Complexities arise because there are a number of independent approaches that can be used to calculate gas saturation. This study will focus on the assessment of gas saturation based on the cased hole data and calculation of saturation from resistivity logs, which were acquired in the open-hole, when the well was drilled.

Schlumberger's PNX™ tool is a recent development in cased hole reservoir surveillance technology. It provides a novel type of measurement, which is sensitive to gas and not to fluid, that can be interpreted to derive an actual saturation value.

The Uithuizen-1 well was selected as a suitable candidate for PNX™ data acquisition, to complement the historical open-hole logs that were acquired at the time of drilling. UHZ-1 was drilled in 1978 as an observation well located in the North of the field, close to the earthquake-prone Loppersum area. By the time the well was drilled, around 650Bcm of gas was produced. As an average over the field, this equates to roughly 22% depletion with respect to initial pressure. It is possible that depletion of the aquifer has impacted the gas saturations below the gas water contact at the moment when the open-hole data was acquired.

Historically, the well has been periodically used to measure reservoir pressure and potential water encroachment. The presence of gas below the contact was already observed from the initial open-hole log evaluation, however, gas saturation values were within the possible saturation measurement uncertainty.

2 Cased hole saturation evaluation

2.1 Pulsed Neutron Logging

The assessment of hydrocarbon saturation in cased holes has long been established by using pulsed neutron logs. Pulse neutron logging (PNL) measures the thermal decay time of a neutron, bombarded into a formation (Morris, et al. 2005). PNL uses a source (minitron), generating 14 MeV neutrons, which is turned on and off (pulsed). During the time the minitron is off, the thermal-neutron or capture gamma-ray counts are measured. The thermal-neutron population is created during the burst and dies away after the end of the burst, due primarily to the capture of these neutrons by nucleus (Figure 2).

The interaction of neutrons with the formation can be described in three stages:

- **Inelastic neutron interaction** – A neutron scattering reaction occurs when a target nucleus emits a single neutron after neutron-nucleus interaction. During an inelastic scattering the neutron is absorbed and then re-emitted. Some energy of the incident neutron is absorbed to the recoiling nucleus and the nucleus remains in the excited state.
- **Elastic neutron interaction** - In elastic scattering reaction between neutron and a target nucleus, there is no energy transferred into nuclear excitation.
- **Neutron absorption** - After a neutron is slowed down as slow as the surrounding matter, the neutron is available for absorption. When a nucleus absorbs the neutron becomes excited, typically emitting capture gamma rays when returning to a stable state. Afterward emitted gamma rays are recorded by the tool detector.

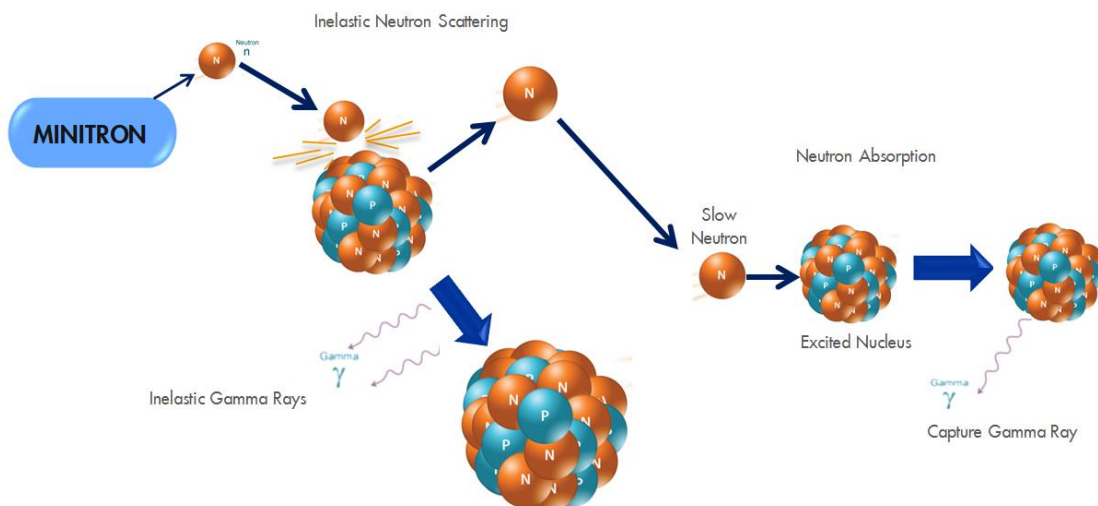


Figure 2: Neutron-Nucleus interaction (courtesy of Schlumberger and mirion.com)

2.2 New developments in logging – Pulsed Neutron Extreme

The recently introduced pulsed neutron logging tool (PNX™) allows to meet today's challenges of quantitative assessment of hydrocarbon saturation in cased hole environment by providing an extended set of independent measurements, namely Sigma, neutron porosity, fast-neutron cross section, and elemental concentrations.

Sigma

Sigma (SIGM) is used to differentiate between hydrocarbon and saline water, since chlorine has a very large capture cross section compared to hydrocarbon and reservoir rock. The greater the total salt count (NaCl per 1000 ppm) in

the formation waters, the better the PNL tool describes the water saturation. SIGM is sensitive to the effect of water salinity, porosity, and shaliness of the rock and matrix composition (Morris et al.,2005). The main uncertainty in the application of SIGM is the definition of the rock matrix values, which vary with lithology variations. Clay will typically have a relatively high Sigma value, and thus can be a large source of inaccuracy if its volume, composition and endpoint are not well defined or fluctuate (Zhou et al.,2016).

FNXS

The new generation of pulsed neutron logging tool are now able to register a new formation nuclear property, the fast neutron cross section (FNXS), that was recently introduced in the logging industry (Rose et al.,2015). The novelty of FNXS is to assess the formation's ability to interact with the fast neutrons. It is very sensitive to gas-filled porosity, while insensitive to liquid-filled porosity (Zhou et al.,2016). The measurement is derived from total gamma-ray counts originating from inelastic interactions and is sensitive to the formation's characteristic to attenuate high energy neutrons (Rose et al.,2015). It is effective for distinguishing gas from rock matrix and fluids. Its response doesn't correlate to hydrogen index (Zhou et al., 2016).

TPHI

TPHI is a pulsed neutron version of a neutron porosity that is similar in response to the open hole dual detector neutron tool. It responds primarily to hydrogen content. TPHI is the most susceptible to differentiate hydrogen liquids such as water and oil from the non-clay rock matrix, which typically contains no hydrogen. Clay is a complicating factor since it contains hydrogen and can lead to inaccuracy if its volume and response are not accurately compensated for (Zhou et al.,2016).

Capture spectroscopy

Capture spectroscopy is used in cased hole to solve for complex lithology. Most of the key elements commonly present in sedimentary rocks, such as Ca, Si, S, Fe, and Al can be measured with capture spectroscopy. Elements are typically given as dry weight concentrations. These elements can be converted to dry weight mineralogy through various methods, e.g. approach by Herron (Herron et al., 1996). If the lithology is unknown, this measurement is very useful in establishing the elemental and mineral composition of the rock.

2.3 PNX™ data acquisition and processing workflow

Pulsed Neutron Xtreme (PNX™) service was recorded for lithology and saturation across the target interval. To meet the specific UHZ-1 job objectives the hybrid logging mode (so called GSH_Lith mode) was selected. This logging mode enabled simultaneous acquisition of time (SIGM, TPHI and FNXS) and energy (spectroscopy) domain data.

Once the raw data was acquired, extra post processing was performed to compensate all data for borehole environment and the completion components. The main steps of the raw data processing are listed in the workflow below (Figure 3).

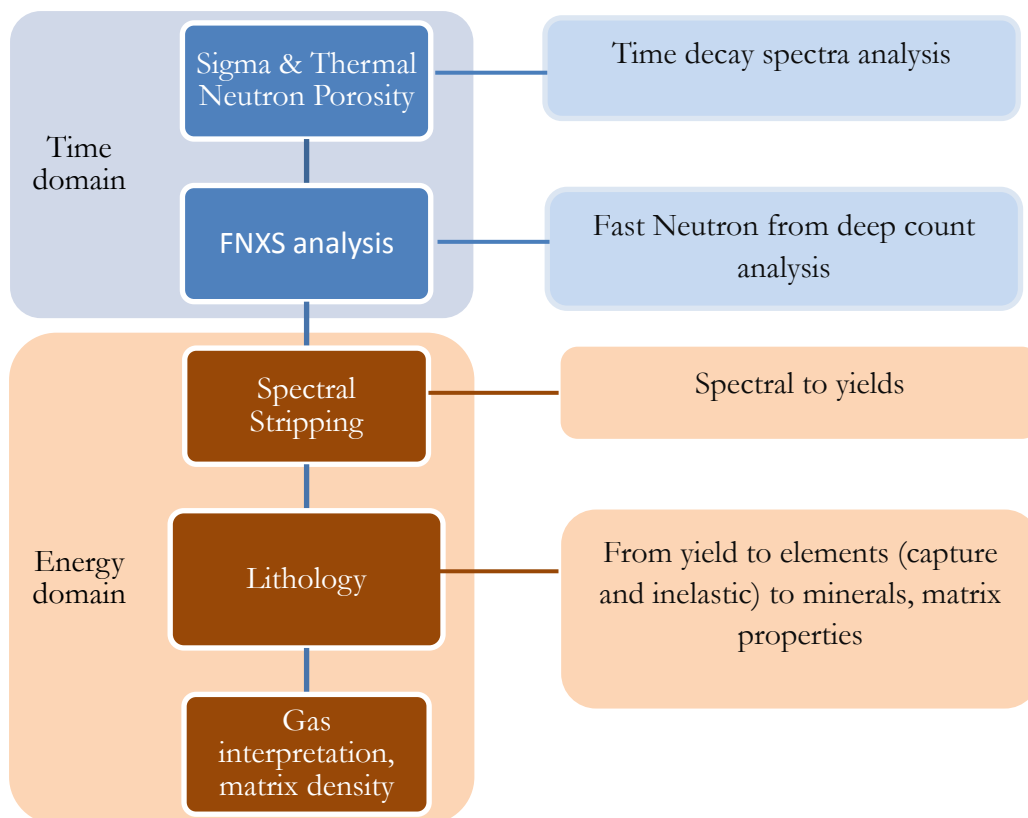


Figure 3: PNX™ raw data processing workflow (courtesy of Schlumberger)

Time domain measurements were used to compute auto-compensated neutron porosity (TPHI), capture cross section (SIGM) and the novel fast neutron cross section (FNXS). All cased hole measurements were self-compensated for borehole environmental effects and completion components.

The first step in the energy domain processing was to get the inelastic and capture elemental yields. Afterwards, the raw elemental yields from the near and far detectors were converted to dry weight elements (capture and inelastic) using a closure model developed at SDR (Schlumberger Doll Research centre).

3 Quantitative saturation assessment

3.1 General method

The general methodology for the determination of hydrocarbon saturation in cased hole is to use a single pulsed neutron measurement, such as SIGM or TPHI in order to solve for two-phase hydrocarbon saturation. This methodology is acceptable for straightforward cases, such as a gas column in a clean rock. As soon as more complex questions arise, a more comprehensive approach should be adopted to provide quantitative results.

The general methodology is to develop a series of measurement response equations as well as to solve for unknown formation volumes (Rose et al., 2017). Formation volumes can be distinguished into two main groups: rock matrix and fluids. Further subdivision may be required based on the complexity of the rock and difference in the fluid system. A generic volume in siliciclastic reservoirs are “sand” and “clays”. For simple interpretation cases the following subdivision is sufficient. However, for a quantitative assessment of gas saturation in the aquifer a more comprehensive multiminerall petrophysical analysis is required.

3.2 Multiminerall petrophysical analysis for complex cases

Multiminerall petrophysical analysis (MMPA) is performed in a specially designed program for quantitative formation evaluation (the Quanti Elan program within the Techlog software by Schlumberger) of cased and open-hole log data. Evaluation is done by optimizing simultaneous equations described by one or more interpretation models. The relationship is often presented in a triangular diagram (Figure 4), where **t** -input log data, **v** - formation component volumes, **R**- responses of 100% formation component (rock, fluid, etc.).

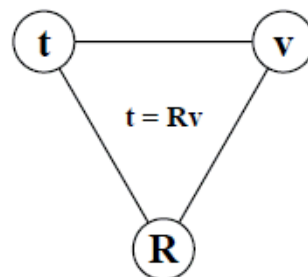


Figure 4: Petrophysical model used by Quanti.Elan application (courtesy of Schlumberger)

MMPA uses both inverse and forward modelling. Inverse modelling is applied to compute only volumes of the formation components. Forward modelling, also known as log reconstruction, computes synthetic curve, based on **v** and **R**. By comparison of synthetic log responses to the actual log data the quality control assessment of a petrophysical model is performed (Techlog™ help files).

The interpretation model consists of set of response equations, a set of formation components, a set of parameters and constraints. Formation components define the minerals, rocks, and fluids, which volumetric outputs are required. It is required that selected components are aligned with the geological description of the formation to which the model is applied. Minerals are solids, which are characterized by a unique chemical formula, for example calcite -CaCO₃. Rock is a natural substance, a solid aggregate of one or more minerals (Wikipedia), such as sedimentary, metamorphic, and igneous.

Response equations are the equations to be solved and their associated input data and uncertainties. The equations describe the logging data. Parameters are the global and program control parameters, response parameters, binding parameters, and salinity parameters. Constraints are the limits that the volumetric results must conform to. They used to set the dependencies between one formation component and another. Constrains are a way to support MMPA modelling with local geological knowledge (Techlog™ help files).

4 Estimation of the mineralogy composition

4.1 Introduction

The mineral composition of the Rotliegend reservoir of the Groningen has been reviewed by Visser (Visser, 2016). This work includes an inventory of all the mineralogical and petrographical analyses carried out on Groningen core material to date.

The bulk mineralogy of the rocks has been determined with whole-rock X-ray diffraction analysis (XRD). This data has been acquired for multiple cored wells in the Groningen area (Figure 5). Quartz is the most abundant mineral, followed by feldspars (plagioclase and K-feldspar), clay minerals (illite-smectite, kaolinite and chlorite) and carbonates (mainly dolomite). The relative abundance of these minerals varies over the extent of the field:

- The ratio of total feldspar to quartz varies from South to North and from base to top of the Slochteren Sandstone
- Authigenic clay mineralogy in the South is dominated by kaolinite and in the North by chlorite and kaolinite
- Trends in the abundance of clay minerals and carbonates are partly controlled by facies. Finer-grained and clay-rich sediments tend to contain higher amounts of illite (plus illite-smectite) and dolomite.

These observations are relevant for the MMPA of logs from well UHZ-1. Analogue wells should preferentially be located at limited distance to avoid bias from fieldwide trends. Figure 5 shows the location of UHZ-1 together with all cored wells with at least 10 whole-rock XRD analyses available. The three wells closest to UHZ-1 are ZRP-3A, ODP-1 and UHM-1A. Bulk mineralogy is available from these wells for both the Upper and the Lower Slochteren Sandstone, and for both the gas leg and the aquifer.

The MMPA approach followed in this document requires as an input the relative composition of the rock matrix, but split up in a sand component and a clay component. The sand component includes detrital grains and pore-filling cements. The clay component includes both detrital and authigenic clay minerals.

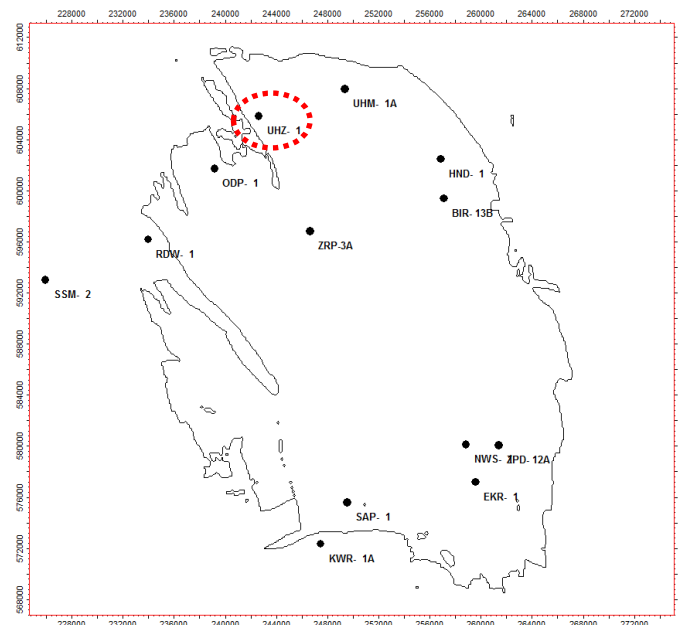


Figure 5: Outline of the Groningen field with location of study well UHZ-1 and surrounding wells with core coverage

4.2 Sand components

The composition of the sand component is shown in Figure 6. Data for wells ZRP-3A and ODP-1 are very comparable. Samples from the aquifer contain circa 88% quartz, 10% feldspar and 2% dolomite, the composition of the gas samples is circa 80% quartz, 17% feldspar and 3% dolomite.

Well UHM-1A has 45 out of 54 samples taken from the water leg. The average composition of these 45 samples is 72% quartz, 16% feldspar and 12% dolomite, which is different from the water leg samples in the other two wells. It is not clear whether or not these differences are real or caused by, e.g., different analytical procedures. For example, the petrography report on UHM-1A is dating from 1969 and reports an “approximate” mineral composition in multiples of 5 percent points (Rahdon, 1969). The petrography work on ODP-1 was carried out in 2003 and on ZRP-3A in 2016, both reporting with 1 percent point accuracy. This suggests that higher confidence should be assigned to the ODP and ZRP data compared to the UHM-1A data.

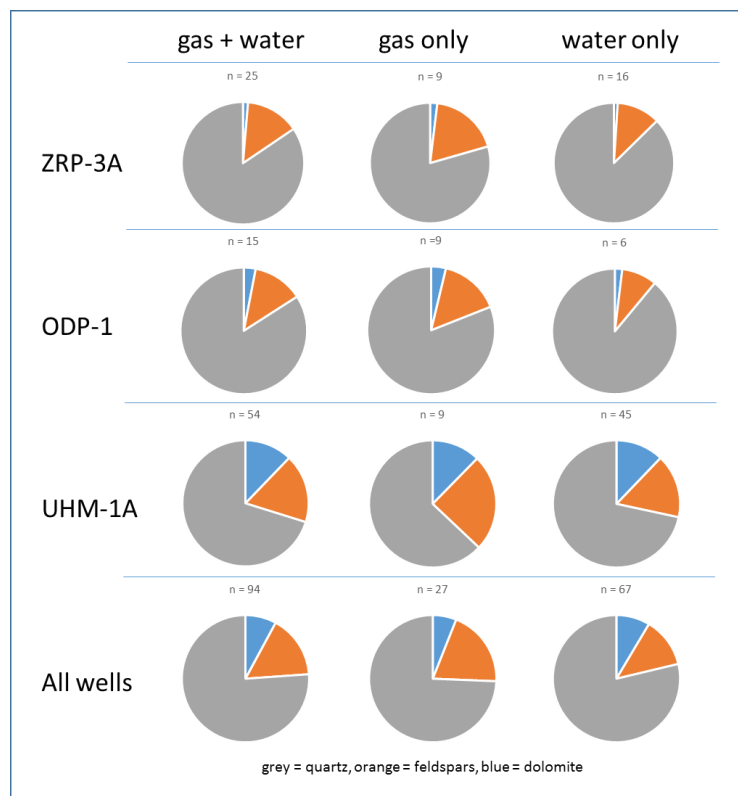


Figure 6: Composition of the sand component of three offset wells for UHZ-1, split per well and per fluid zone. Data obtained from whole-rock XRD analysis

Based on the above data for ZRP-3A and ODP-1 only, an average composition of the sand content in well UHZ-1 is estimated at (Figure 6):

- Quartz: 80%
- Feldspar: 17%
- Dolomite: 3%

4.3 Clay components

Total clay from whole-rock XRD analysis in well ZRP-3A is 8%, almost evenly split between chlorite, illite/smectite and kaolinite. For well ODP-1 this is 16%, half of which is illite/smectite and the other half split between chlorite and kaolinite. The composition of clay minerals based on clay-fraction XRD is shown in Figure 7. The two methods yield

fairly comparable results, taking into account the limited number of samples analyzed, the different sample preparation techniques and the facies dependence of the clay minerals.

Based on this, the composition of the clay component in well UHZ-1 is estimated at (Figure 8):

- Illite/smectite: 40%
- Chlorite: 30%
- Kaolinite: 30%

The whole-rock and clay-fraction XRD data for UHM-1A is of lower confidence but indicates a very comparable composition.

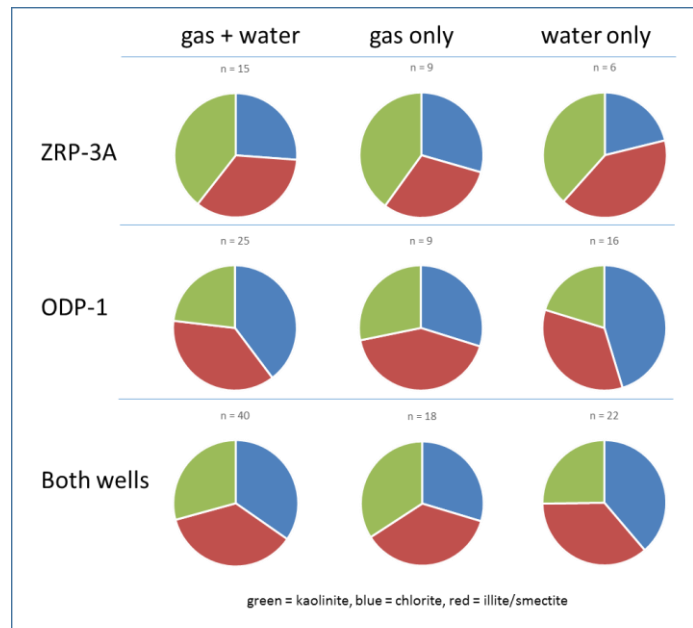
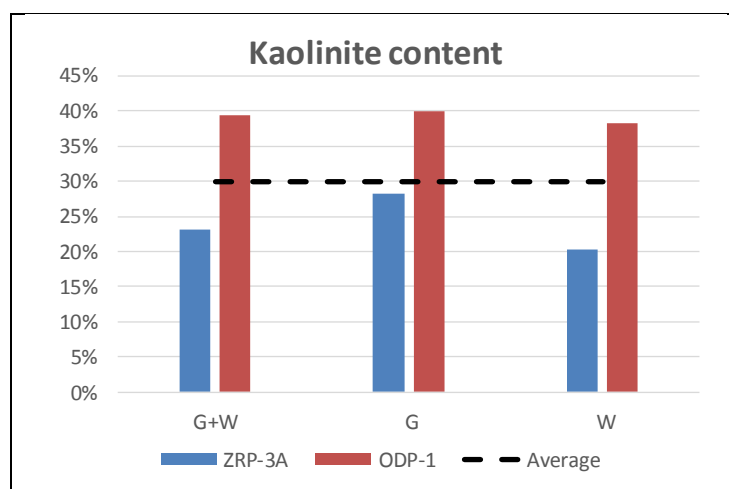


Figure 7: Composition of the clay component of two offset wells for UHZ-1, split per well and per fluid zone. Data obtained from clay-fraction XRD analysis.



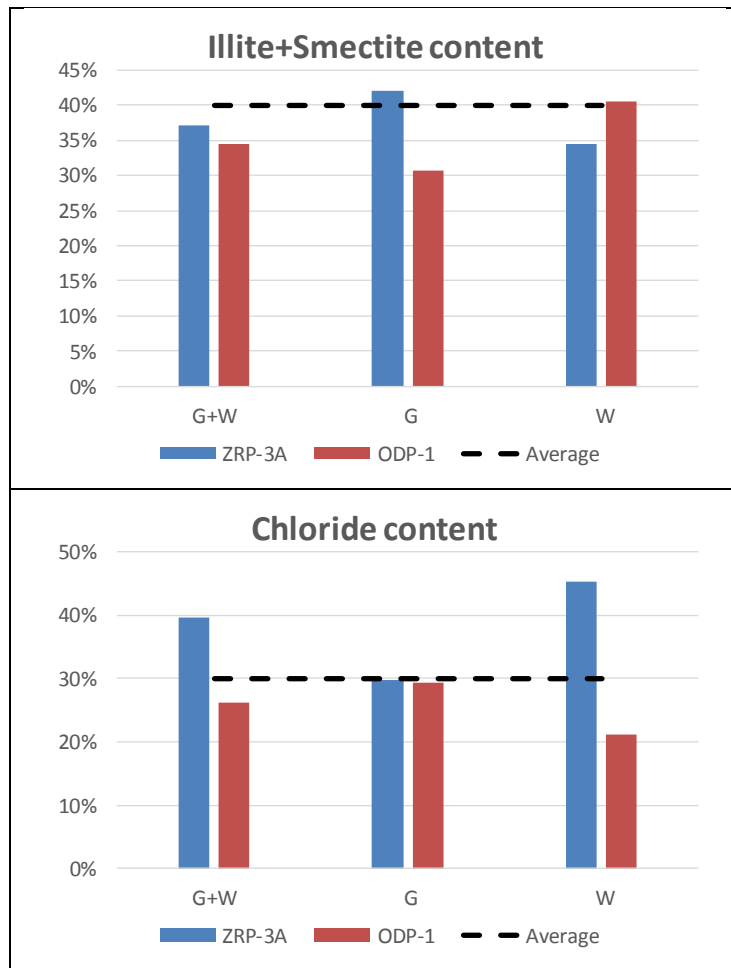


Figure 8: Average composition of the clay components for offset wells and UHZ-1

5 Uithuizen-1 FNXS analysis

As discussed in section 2.2, the FNXS measurement is based on fast neutrons, which are indirectly measured through the detection of induced inelastic gamma rays by the logging tool. This is done using a designed type of detector (deep PNX YAP) coupled to an optimized source neutron pulsing scheme used by PNX™. The response of the inelastic gamma rays count rate is modelled in a wide range of cased hole environments. More details with regards to the subject are given in Appendix 1.

FNXS -TPHI cross plot is used to differentiate intervals filled with gas and water. The main application of the plot is similar to a neutron-density cross plot, that is widely used in open-hole formation evaluation.

Figure 9 illustrates the approach of identifying gas filled intervals based on FNXS-TPHI cross plot.

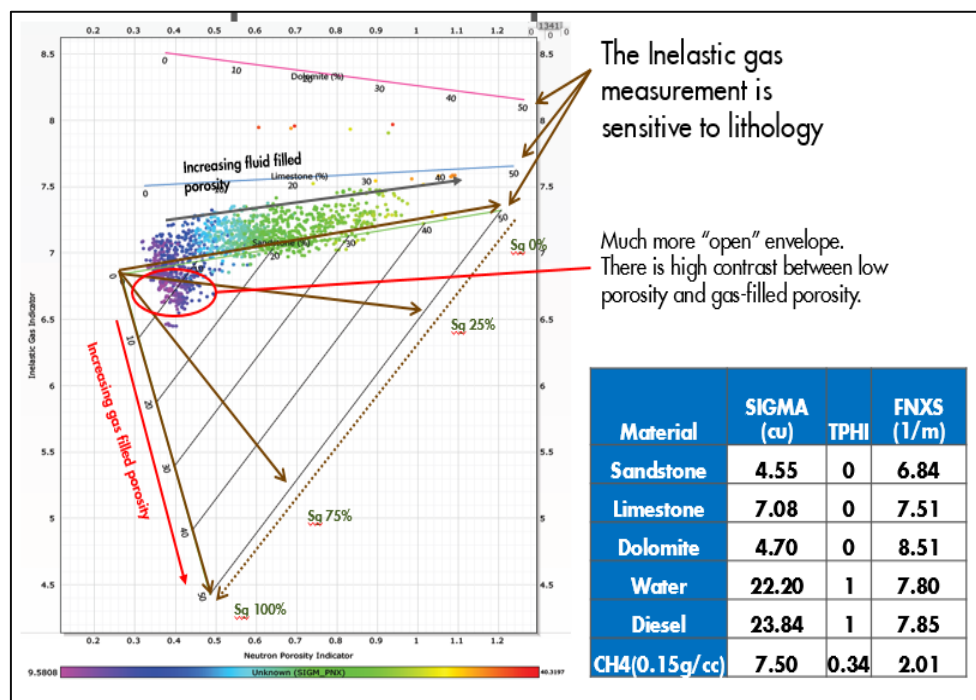


Figure 9: Example of interpretation envelope of FNXS measurement (courtesy of Schlumberger)

The same approach is used to analyse the UHZ-1 PNX™ logging data. As displayed below (Figure 10), the whole logged interval can be subdivided into three zones based on TPHI-FNXS responses: gas filled (green), residual gas (orange) and water zone (blue). The cloud of green points indicates the gas filled interval and is characterized with low FNXS responses. The blue cloud represents the water zone and is characterized with high FNXS responses. The orange zone between gas and water represents the residual gas.

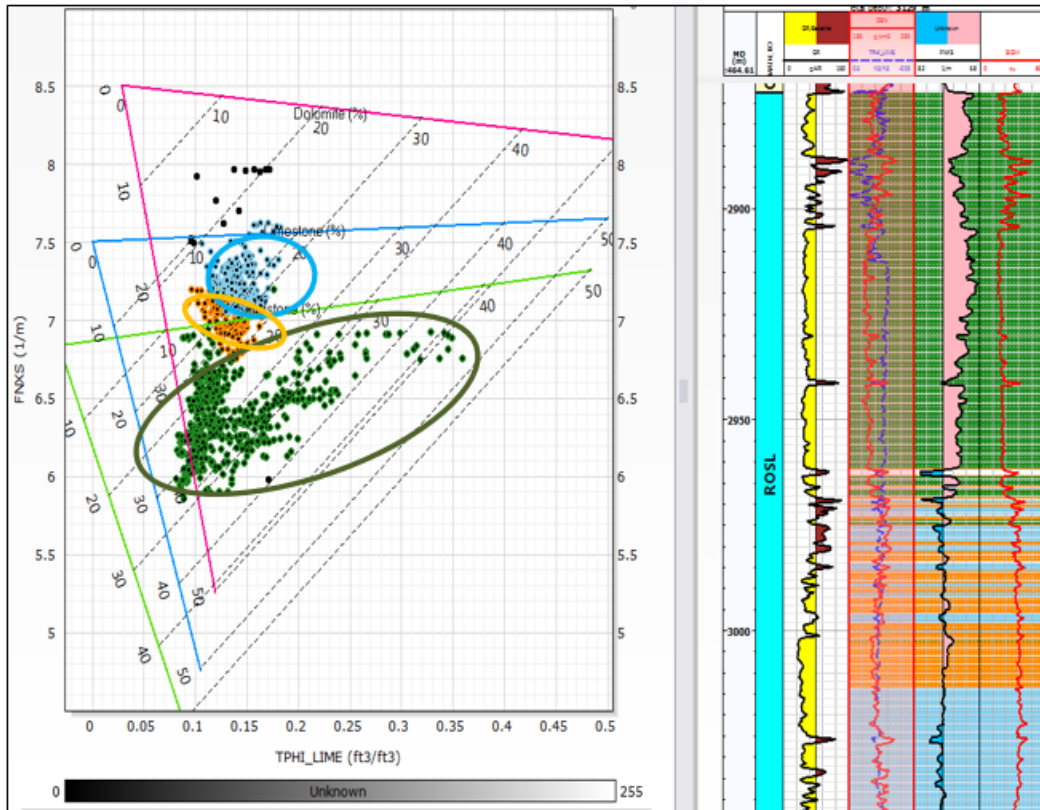


Figure 10: UHZ-1 FNXS analysis (the shading on the log tracks corresponds with the coloured points in the cross plot)

- Track 1- Depth reference (measured depth), m AHORT (original rotary table)
- Track 2- Zonation name
- Track 3- Open-hole Gamma Ray log
- Track 4- Open hole bulk density and TPHI overlay for gas zone identification.
- Track 5- FNXS log, displayed in inverted scale (8.2-5.8), low values represent gas (rose fill), high values represent water/rock (blue fill)
- Track 6- SIGM log

The technique of cross plotting FNXS and TPHI indicated the existence of residual gas below the initial gas water contact (GWC). However, the above approach allows only for qualitative assessment, for quantitative evaluation the MMPA modelling was utilized.

6 Multi-Mineral Petrophysical Analysis for cased hole evaluation

MMPA involves the construction of a mineral model as a simplified representation of reality. All formation evaluation problems are vastly underdetermined. It is unlikely that anyone will ever have enough measurements, with sufficient accuracy and resolution in all dimensions, to fully describe the near-wellbore environment.

As was discussed in Chapter 4, the mineral composition of Rotliegend is complex. An accurate assessment of clay volume is critical in determination of the reservoir properties from logs. The most important properties are porosity and saturation. To address the complexity of clay and rock composition the multiminerale petrophysical model is required.

Acquisition of PNX data allows to build a complex model and assess volumes of clay minerals, rock components and fluids. However, the understanding of clay minerals distribution across the Groningen field as wells as rock minerals distribution and its vertical variability should be incorporated into the model as a way to introduce geological knowledge.

MMPA analysis is designed to evaluate interval below the GWC and incorporates FNXS, SIGM, TPHI, spectroscopy and open hole density data into one interpretation model. Each data input is used to quantify either matrix, shale or fluid components. The parameter initialization step is required for MMPA run.

6.1 Parameter initialization

The parameter initialization step is required to arrive at parameters for water and gas, which depend on actual pressure as well as temperature data varying with depth. Knowledge of water salinity and expected formation porosity are also essential for calculating formation water density, conductivity and other parameters, which are required for MMPA. The detailed list of main input and output curves can be found in the Appendix 3.

Table 1 illustrates input parameters for the UHZ-1 well. The salinity estimate was taken from the previous petrophysical study (Van der Graaf, Seubring, 2003).

Table 1: UHZ-1 parameter initialization inputs

Zone	ROSL_GAS	ROSL_RES_GAS
Top	2872.5	2968
Bottom	2968	3104
MFST (degC)	-9999	-9999
RMF (ohm.m)	-9999	-9999
XWaterSalt (kppm)	320	320
RWT (degC)	-9999	-9999
RW (ohm.m)	-9999	-9999
UWaterSalt (kppm)	320	320
Water Based Mud	no	no
Average Por (v/v)	0.2	0.2

6.2 Main model setup

The input table represents the list of log data that are used in the interpretation process with associated measurement uncertainties (Table 2). The amount of log inputs must at least be equal to the number of unknown formation components, otherwise the system is undetermined. If the amount of log inputs exceeds the number of unknowns, the system is overdetermined, and some means must be utilized to settle any disagreements among the equations. The number of unknown can never exceed the total number of input log data, otherwise the system is undetermined.

Table 2: MMPA input channels and uncertainties

	Family	Uncertainties	Uncertainty Type	Input Weight	Unflushed factor	Equation type	Tool type	Constants	Activate
1	Neutron Porosity	0.015	Absolute	0.8	0	Linear	NPHI	Neutron Porosity	yes
2	UI_Aluminum Weight Fraction	DWAL_SIG_INCP	Absolute	1	0	Dry Weight		Aluminum Weight Fraction	yes
3	UI_Calcium Weight Fraction	DWCA_SIG_INCP	Absolute	1	0	Dry Weight		Calcium Weight Fraction	yes
4	UI_Potassium Weight Fraction	DWK_SIG_INCP	Absolute	1	0	Dry Weight		Potassium Weight Fraction	yes
5	UI_Silicon Weight Fraction	0.01	Absolute	1	0	Dry Weight		Silicon Weight Fraction	yes
6	UI_Sulfur Weight Fraction	DWSU_SIG_INCP	Absolute	1	0	Dry Weight		Sulfur Weight Fraction	yes
7	UI_Iron Weight Fraction	DWFE_SIG_INCP	Absolute	1	0	Dry Weight		Iron Weight Fraction	yes
8	UI_Magnesium Weight Fraction	DWMG_SIG_INCP	Absolute	1	0	Dry Weight		Magnesium Weight Fraction	yes
9	UI_FNXS	FNXS_SIG	Absolute	1	0	Linear			yes
10	UI_Formation Sigma	0.1	Absolute	1	0	Linear		Formation Sigma	yes
11	Bulk Density	0.027	Absolute	1	0	Linear		Bulk Density	yes
12	UI_Titanium Weight Fraction	DWTL_SIG_INCP	Absolute	1	0	Dry Weight		Titanium Weight Fraction	yes

For an overdetermined system, it is necessary to apply a weight factor. A weight factor of 1.0 means the log measurement will impact the model results significantly. If all input logs have the same weight factor, it means that each log has an equal effect on the results. However, some log data can be more relevant or of better quality compared to other data and thus, the weight factor might need to be adjusted. Figure 12 illustrates the overdetermined systems with applied weights (Quanti Elan theory, Techlog™ helpfiles).

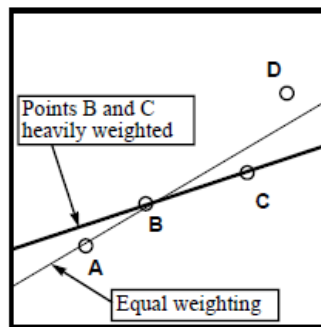


Figure 12: Overdetermined system with applied weights (courtesy of Schlumberger)

All measurements are subject to uncertainty and a measurement result is complete when it is accompanied by a statement of the associated uncertainty. Uncertainty reflects the incomplete knowledge of the quantity value (JCGM 100, 2008). Measurement uncertainty should not to be confused with measurement error. The average values of PNX measurement uncertainties are provided in the Table 3.

Table 3: Average uncertainties from PNX processing for the studied interval

Element	Average uncertainty	Element	Average uncertainty
Aluminium	0.01	Sulphur	0.01
Calcium	0.019	Iron	0.006
Potassium	0.01	Magnesium	0.017
Silicon	0.01	FNXS	0.025

A response equation (equation type) is the mathematical description of how a given measurement varies with respect to each formation component. The simplest linear response equations are of the form:

$$Measurement = \sum_{i=1}^n V_i * R_i$$

where:

V_i – volume of formation component i

R_i – response parameter for formation component i

However, certain linear equations include additional terms, and the nonlinear equations are more complex. The overall concept is the same: the total measurement observed is determined by the volume of each formation component and how the tool reacts to that formation component (Techlog™ helpfile).

6.3 Formation components

The response equations previously described require input for fluids and rock or minerals parameters to function. There are no default values for rocks as they are composed of undefined mixtures of minerals. Minerals, in turn, have a definite chemical structure and its parameters are more well-known. For example, there is very little debate over the composition of quartz. Clay minerals, though, are more complex. The fluid parameters are dependent on hydrocarbon type and water salinity. The parameter initialization step (section 6.1) is used to determine the different fluid parameters.

The component specification table (Table 4) provides most of the parameter values required to run a MMPA. The minerals selection is based on petrographic analysis of Groningen core samples and was discussed in Chapter 4. The table gives the endpoint parameters, the value that would be registered by a logging tool if it was surrounded by an infinite amount of a 100% pure mineral or fluid. For example, if the density tool will be logged in 100% pure quartz, the registered bulk density value will be equal to 2.65 g/cc. Those elemental dry weight end-points are default values loaded from the global database. Some default values in the database were updated according to work done by Schlumberger-Doll Research centre and documented by M.M. Herron and A. Matteson in their paper (Herron, Matteson,1993).

Table 4: Formation components list and end-points

Input properties	Component Specification		Wet clays	Special Models	Additional constraints		Post-process parameters			Uncertainties	
	Illite	kaolinit	mectit	hlorit	Quartz	Feldspal	Dolomite	XWater	XGas	UWater	UGas
Activate	yes	yes	yes	yes	yes	yes	yes	yes	yes	yes	yes
Bulk Density (g/cm3)	2.735	2.63	2.78	3.01	2.65	2.57	2.87	1.17	0.058	1.17	0.058
Neutron Porosity (v/v)	0.361	0.37	0.218	0.52	0.06953061	0.02	0.05553411	1	-0.027	1	-0.027
Porosity (v/v)	0	0	0	0	0	0	0	1	1	1	1
UI_Aluminum Weight Fraction (lbf/lbf)	0.105	0.095	0.091	0.096	0	0.099	0.001	0	0	0	0
UI_Calcium Weight Fraction (lbf/lbf)	0.005	0.001	0.014	0.007	0	0.001	0.216	0	0	0	0
UI_Potassium Weight Fraction (lbf/lbf)	0.045	0.001	0.00658	0.004	0	0.102	0	0	0	0	0
UI_Silicon Weight Fraction (lbf/lbf)	0.248	0.208	0.264	0.14	0.4675	0.3	0.006	0	0	0	0
UI_Sulfur Weight Fraction (lbf/lbf)	0	0	0	0	0	0	0.001	0	0	0	0
UI_Iron Weight Fraction (lbf/lbf)	0.022	0.004	0.02	0.208	0	0.001	0.01	0	0	0	0
UI_Magnesium Weight Fraction (lbf/lbf)	0.012	0.001206	0.022	0.048	0	0.001	0.123	0	0	0	0
UI_FNXS	7.4	7.9	8.2	8.2	6.84	6.33	8.51	7.15	0.772	7.15	0.772
UI_Formation Sigma (CU)	42	24	22	43.7	4.7	15.3	6.92	148.8524	2.881	148.8524	2.881
UI_Titanium Weight Fraction (lbf/lbf)	0.005	0.011	0.001	0.013	0	0	0	0	0	0	0
Permittivity	5.8	5.1	5.5	5	4.65	5.3	6.8	40.46292	1	40.46292	1
Conductivity (mho/m)	0	0	0	0	0	0	0	86.02731	0	86.02731	0
Min Volume	0	0	0	0	0	0	0	0	0	0	0
Max Volume	1	1	1	1	1	1	1	1	1	1	1
MxType	Shale	Shale	Shale	Shale	Matrix	Matrix	Matrix	Xfluid	Xfluid	Ufluid	Ufluid
Salinity (kppm)	0	0	0	0	0	0	0	320	0	320	0

The end-points for SIGM, FNXS and TPHI are not default values, as they depend upon gas density, pressure, and temperature. They should be calculated for each individual case. The end-point results for the mentioned log inputs are listed in the Table 5.

Table 5: End points calculation of SIGM, FNXS, TPHI for the given gas properties (SG, P, T)

Date	Pressure, bar	Gas Density @ 112 degC, g/cc	Gas Density @ 120 degC, g/cc	Source of Gas Density	Top ROSL, at 112 degC				Bottom ROSL			
					Density Gas (g/cm3)	Sigma Gas	TPHI Gas	FNXS Gas	Density Gas (g/cm3)	Sigma Gas	TPHI Gas	FNXS Gas
4/20/2017	97.13	0.059	0.058	MoReS	0.059	2.954	-0.023	0.792	0.058	2.881	-0.027	0.772

6.4 Constraints and Constants

It should be mentioned that within the Quant-Elan model set-up there are two ways of imposing geological or petrophysical information into the interpretation model: through constants and constraints. Constraints are absolute minimum and/or maximum limits on formation component volumes. Unlike constant tools, which are weighted by uncertainties, constraints are absolute limits. They do not represent a curve bound to data and are the means of adding local knowledge to the model through equations. For example, when solving for complex clay system, it is beneficial to incorporate knowledge of clay distribution from near-by wells for more precise model reconstruction.

For example, dolomite-to-quartz ration of the first well is around 5 %, and the geology is similar between two wells. That knowledge can be included into the model as: quartz/dolomite=0.05 or $0=1*\text{quartz}-0.05*\text{dolomite}$. UHZ-1 well has a complex mineral composition and this is reflected through more complicated dependencies in constant tools (Table 6).

It is valid to note that XRD inputs should be represented via constant tool and should not be used as absolute controlling parameters for the model reconstruction due to uncertainties and possible errors associated with core extraction and XRD analysis itself.

Table 6: Constraints and constant tool table

Type	Additional constraints								
	1	2	3	4	5	6	7	8	9
Constraint	Constraint	Constraint	Constant tool	Constant tool	Constant tool	Constant tool	Constant ...	Constant ...	Constant ...
Uncertainty	0.015	0.015	0.015	0.015	0.015	0.015	0.015	0.015	0.015
Weight	1	1	0.15	0.15	0.15	0.15	0.15	0.15	0.15
Constant	0	0	0	0	0	0	0	0	0
Illite	0	0	0.7	-0.3	-0.1	-0.3	0	0	0
Kaolinite	0	0	-0.3	0.7	-0.1	-0.3	0	0	0
Smectite	0	0	-0.3	-0.3	0.9	-0.3	0	0	0
Chlorite	0	0	-0.3	-0.3	-0.1	0.7	0	0	0
Quartz	0	0	0	0	0	0	0.2	-0.17	-0.03
K-Feldspar	0	0	0	0	0	0	-0.8	0.83	-0.03
Dolomite	0	0	0	0	0	0	-0.8	-0.17	0.97
XWater	0	-1	0	0	0	0	0	0	0
XGas	1	0	0	0	0	0	0	0	0
UWater	0	1	0	0	0	0	0	0	0
UGas	-1	0	0	0	0	0	0	0	0
Min Volume	0	0	0	0	0	0	0	0	0
Max Volume	0	0	0	0	0	0	0	0	0

6.5 MMPA main outputs

The logs in Figure 12 illustrate the main MMPA processing results as computed by integrating the PNX™ log data with the open hole bulk density log data (which includes rock volumes, porosity, and saturation). Core data was used to guide the final minerals and clays selection. The logs are restricted to the interval of interest, the water leg below the gas-water-contact.

The primary quality control mechanism for the MMPA results is the reconstructed logs. Reconstructed log quality information is available in two forms: the curve SDR (standard deviation of the reconstruction), and the individual reconstructed logs. The SDR provides an overall indication of how well the logs are reconstructed. The individual reconstruction curves indicate how each curve was reconstructed for given defined formation components. A further quality control mechanism is that the output model should be robust when tested against the regional core and log data.

There is a good correlation and reconstruction between actual log measurements and synthetic modelled curves for the interval of interest. Quality control and sensitivity analysis also confirm that the minerals and fluids selection was proper, as well as inputs for uncertainty and weights.

The following tracks are displayed in Figure 12:

Track 1	Depth reference (measured depth), m AHORT (original rotary table)
Track 2	Zonation name
Track 3	Reconstruction of Titanium dry weight with uncertainty
Track 4	Reconstruction of SIGM response with uncertainty
Track 5-12	Reconstruction of FNXS, Magnesium, Iron, Sulphur, Silicon, Potassium, Calcium, Aluminium dry weight with uncertainties
Track 13	Reconstruction of open hole bulk density with uncertainty
Track 14	Reconstruction of PNX TPHI with uncertainty
Track 15	Comparison of open hole total porosity vs PNX™ model output porosity
Track 16	Cumulated rock and fluid model (colour definition as displayed in the table 4)
Track 17	Rock model
Track 18	Total porosity, inverted scale 0-0.3 v/v
Track 19	Clay corrected porosity, inverted scale 0-0.3 v/v
Track 20	Gas saturation, green area fill, scale 0-1.0 v/v
Track 21	Apparent Matrix density from MMPA (black colour) compared against stand-alone PNX spectroscopy processing (red colour), scale 2.5-3.0 g/cc
Track 22	Volume of shale, scale 0-1.0 v/v
Track 23	SDR, unitless

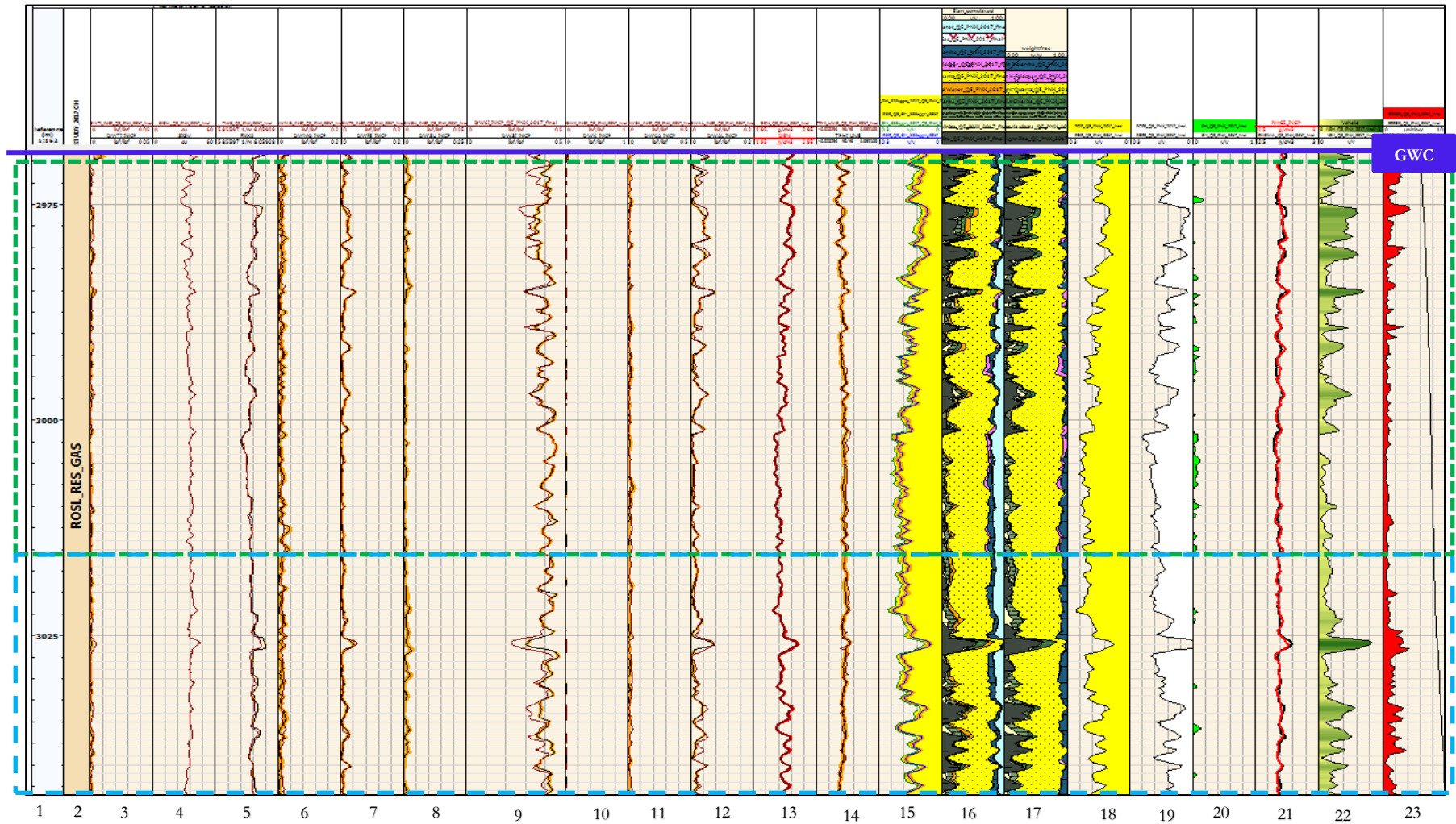


Figure 12: Cased hole MPPA main results (the box highlights difference in gas saturation with depth)

6.6 MMPA cased hole results

A Multimineral Petrophysical Analysis was performed for the cased hole environment across the depth interval below the GWC. Such analysis enables a quantitative assessment of the gas saturation. However, it is important to note that the resulting gas saturation is the best model estimate and does not incorporate an uncertainty assessment of gas saturation to fully quantify the range. It became evident that a full uncertainties analysis around the gas saturation measured through casing is complex. Additional data acquisition and statistical analysis is required to further study the subject.

The main results can be summarized as follows:

- A small quantity of gas was calculated in the interval below the GWC (GWC at 2969 m AHORT)
- A fairly consistent gas signature was observed down to 46 m below the GWC (over the interval from 2969 m AHORT till 3015 m AHORT) with average gas saturation value of around 8-10% with some peaks up to 20%.
- The calculated gas saturation distribution is rather patchy, than continuous.

7 Multi-Mineral Petrophysical Analysis for open hole evaluation

The acquisition of PNX™ spectroscopy data on UHZ-1 helped to improve the mineralogical model of the Rotliegend formation for the well. This allowed for a reassessment of the gas saturation based on the historic open-hole log data. The modelling of open-hole data is similar to the method described in Chapter 6, except that the gas saturation is calculated using formation resistivity inputs and the Waxman-Smiths model with saturation components for the water leg, as described in the current Groningen field petrophysical model (Van der Graaf, Seubring, 2003).

7.1 Parameter Initialization

For open-hole evaluation, the initialization of the parameters should be performed by applying the reservoir conditions at the time the well was drilled. The mud parameters were taken from field log prints and incorporated into the initialization module. The input values are listed in Table 7.

Table 7: UHZ-1 open-hole parameter initialization inputs

Pressure Method	Mud Density	MFST (degC)	18
Drilling fluid density	1.05	RMF (ohm.m)	0.054
Drilling fluid unit	g/cm3	XWaterSalt (kppm)	-9999
Pressure Gradient	9.792	RWT (degC)	-9999
Pressure Gradient unit	kPa/m	RW (ohm.m)	-9999
		UWaterSalt (kppm)	320
		Water Based Mud	yes
		Average Por (v/v)	0.2
		Dielectric Frequency Type	SLB ADT F3
		Dielectric Frequency (Mhz)	-9999

7.2 Main model inputs

Table 8 displays the main input channels for MMPA, their uncertainties and weights.

Table 8: MMPA input channels and uncertainties for OH evaluation

	Family	Uncertainties	Uncertainty Type	Input Weight	Unflushed factor	Equation type	Tool type	Constants	Activate
1	Bulk Density	0.027	Absolute	1	0	Linear		Bulk Density	yes
2	Neutron Porosity	0.015	Absolute	1	0	Linear	NPHI	Neutron Porosity	yes
3	Formation Resistivity	RESUWAT_UNC	Absolute	1	1	Linear			yes
4	Flushed Zone Resistivity	RESXWAT_UNC	Absolute	1	0	Linear			yes
5	UI_Aluminum Weight Fraction	DWAL_SIG_INCP	Absolute	1	0	Dry Weight		Aluminum Weight Fraction	yes
6	UI_Calcium Weight Fraction	DWCA_SIG_INCP	Absolute	1	0	Dry Weight		Calcium Weight Fraction	yes
7	UI_Potassium Weight Fraction	DWK_SIG_INCP	Absolute	1	0	Dry Weight		Potassium Weight Fraction	yes
8	UI_Silicon Weight Fraction	0.01	Absolute	1	0	Dry Weight		Silicon Weight Fraction	yes
9	UI_Sulfur Weight Fraction	DWSU_SIG_INCP	Absolute	1	0	Dry Weight		Sulfur Weight Fraction	yes
10	UI_Iron Weight Fraction	DWFE_SIG_INCP	Absolute	1	0	Dry Weight		Iron Weight Fraction	yes
11	UI_Magnesium Weight Fraction	DWMG_SIG_INCP	Absolute	1	0	Dry Weight		Magnesium Weight Fraction	yes

7.3 Formation components

The list of the minerals and fluids in the model and each component endpoint is shown in the Table 9 (no changes with respect to the cased hole endpoints as described in section 6.3).

Table 9: Formation component end-points for OH evaluation

Input properties	Component Specification				Wet clays	Special Models	Additional constraints	Post-process parameters		Uncertainties	
	Illite	Kaolinit	Smectit	Chlorit	Quartz	Feldspa	Dolomite	XWater	XGas	UWater	UGas
Activate	yes	yes	yes	yes	yes	yes	yes	yes	yes	yes	yes
Bulk Density (g/cm3)	2.735	2.63	2.78	3.01	2.65	2.57	2.87	1.084164	0.157	1.189448	0.157
Neutron Porosity (v/v)	0.361	0.37	0.218	0.52	-0.06953061	0.02	0.05553411	1	0.1816437	1	0.1816437
UI_Aluminum Weight Fraction (lbf/lbf)	0.105	0.204	0.091	0.096	0	0.099	0.001	0	0	0	0
UI_Calcium Weight Fraction (lbf/lbf)	0.005	0.001	0.014	0.007	0	0.001	0.216	0	0	0	0
UI_Potassium Weight Fraction (lbf/lbf)	0.045	0.001	0.00658	0.004	0	0.102	0	0	0	0	0
UI_Silicon Weight Fraction (lbf/lbf)	0.248	0.208	0.264	0.14	0.4675	0.3	0.006	0	0	0	0
UI_Sulfur Weight Fraction (lbf/lbf)	0	0	0	0	0	0	0.001	0	0	0	0
UI_Iron Weight Fraction (lbf/lbf)	0.048	0.004	0.02	0.208	0	0.001	0.01	0	0	0	0
UI_Magnesium Weight Fraction (lbf/lbf)	0.012	0.001206	0.022	0.048	0	0.001	0.123	0	0	0	0
UI_Titanium Weight Fraction (lbf/lbf)	0.005	0.011	0.001	0.013	0	0	0	0	0	0	0
Permittivity	5.8	5.1	5.5	5	4.65	5.3	6.8	42.24662	1	41.18543	1
Conductivity (mho/m)	0	0	0	0	0	0	0	65.77645	0	86.5956	0
Min Volume	0	0	0	0	0	0	0	0	0	0	0
Max Volume	1	1	1	1	1	1	1	1	1	1	1
MxType	Shale	Shale	Shale	Shale	Matrix	Matrix	Matrix	Xfluid	Xfluid	Ufluid	Ufluid
Salinity (kppm)	0	0	0	0	0	0	0	187.1586	0	320	0

7.4 Wet Clay Model

To account for clay bound water in the Waxman-Smiths saturation model, the wet clay inputs are required. The parameters listed in Table 10 are extracted from the default database and calculated for the relevant temperature and pressure at UHZ-1.

Table 10: Wet clay component end-points for OH evaluation

	Illite	Kaolinite	Smectite	Chlorite
Wet Clay Porosity (v/v)	0.09129252	0.05154075	0.3895858	0.09391999
Rsh (ohm.m)	3	7	0	5
CEC (meq/g)	0.16	0.09	1	0.15
CBW (mho/m)	37.2869	37.2869	37.2869	37.2869
Bulk Density (g/cm3)	2.594	2.556	2.16	2.839
Neutron Porosity (v/v)	0.419	0.402	0.523	0.565
UI_Aluminum Weight Fraction	0.095	0.193	0.056	0.087
UI_Calcium Weight Fraction	0.005	0.001	0.009	0.006
UI_Potassium Weight Fraction	0.041	0.001	0.004	0.004
UI_Silicon Weight Fraction	0.225	0.197	0.161	0.127
UI_Sulfur Weight Fraction	0	0	0	0
UI_Iron Weight Fraction	0.044	0.004	0.012	0.188
UI_Magnesium Weight Fraction	0.011	0.001	0.013	0.043

7.5 Saturation Model

7.5.1 Waxman-Smits saturation method

Water saturation determination is the most challenging of petrophysical calculations, especially if such assessment is required for shaly sandstones, like the Rotliegend. The most common used shaly sand water saturation model is the Waxman-Smits (W-S) model. The W-S model principles are available in the public domain and described in great details by many authors (Waxman et al.,1968,1974)

The W-S water saturation formula is listed below:

$$S_w^{n^*} = \frac{R_w}{\phi^{m^*} R_l \left[1 + R_w B \frac{Q_v}{S_w} \right]}$$

where:

R_l	formation resistivity, ohm-m
Q_v	cation exchange capacity per unit pore volume, eq/L
ϕ	calculated total porosity, v/v
m^*	Waxman-Smits cementation exponent
n^*	Waxman-Smits saturation exponent
R_w	formation water resistivity, ohm-m
B	equivalent cationic conductance of a sodium ion

The W-S model addresses the clay effect while calculating the water saturation. There are two properties of clay minerals that contribute to the problem of calculating water saturation in clay bearing sandstones: surface area and cation exchange capacity (CEC) (Pittman,1989). Authigenic clay minerals, especially those with the fibrous morphology (e.g. illite), possess a very high surface area. If the rock is water-wet, then the surface of the clay is covered by a 1 or 2-molecule thick layer of water. The micropores among clay particles also hold water by capillary retention forces. The water absorbed by the clay and held in the micropores is considered to be “bound water”.

The amount of bound water is dependent both on the morphology and CEC of the clay minerals. The table below represents values of CEC and cation exchange capacity per unit total pore volume (Q_v) for different clay minerals, as used in the Waxman-Smits equation for the saturation evaluation.

Table 11: CEC and Q_v values for different clays minerals

Clay Mineral	CEC (meq/100g)	Q_v (meq.cm-3)
Kaolinite	2-15	0.015-0.12
Chlorite	0-40	0.052-0.24
Illite	10-40	0.051-0.22
Smectite	76-150	0.34-0.81

The ranges as outlined in Table 11 are a result of the variability of clay minerals within the reservoir, and various abilities of the clays to “hold” water. It’s crucial to have an accurate assessment of individual clays in Slochteren formation. The main clay morphotypes of the Rotliegend were identified in the study of the NE Netherlands (Kelly, S., Greenwood, J., 1996) by SEM photomicrographs, and are presented in Figure 13.

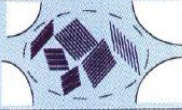

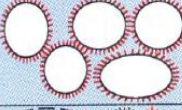
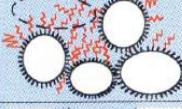


CLAY MINERAL	CODE	APPEARANCE
KAOLINITE	K1 (COARSE VERMIFORM)	
KAOLINITE	K2 (FINE BLOCKY & VERMIFORM)	
KAOLINITE	K3 (ABUNDANT PORE FILLING AGGREGATE)	
ILLITE	I1 (GRAIN COATING BOXWORK)	
ILLITE	I2 (FIBROUS EXTENSIONS)	
ILLITE	I3 (BLADED IN DISSOLUTION PORES)	
CHLORITE	C1 (GRAIN COATING BOXWORK)	
CHLORITE	C2 (COARSE EUHEDRAL PLATES AND ROSETTES)	

Figure 13: Main clay morphotype identified in the clay mineral diagenesis study in the Rotliegend of the NE Netherlands (Kelly, Greenwood, 1996)

7.5.2 Waxman-Smits saturation parameters inputs

The saturation model was reviewed in detail as part of the 2003 Groningen Field Review (Van der Graaf, Seubring, 2003). The petrophysical review was mainly focusing on the assessment of the saturation parameters for the gas zone. However, a rough estimate of saturation parameters for the water leg was performed. From the foregoing, it is clear that a more detailed study of the issue will be required and, as a result, some changes in the saturation parameters for the water zone will have to be applied.

The saturation coefficients for the water zone as derived in the 2003 review are listed below (Table 12).

Table 12: Waxman-Smits saturation coefficients

	Deep Res Method	Deep a	Deep m	Deep n	Deep Resistivity		Compute Qv	Deep B method
					Water Resistivi	Temperature (
1	Waxman-Smits	0.64	2.2382	2.095	0.01173305	118.0599	1	1978 Waxman B chart

7.6 Constraints and Constants

Constraints and constants are identical to those described in section 6.4.

7.7 MMPA main outputs

The log plots below (Figure 14) illustrate the main open-hole MMPA processing results, with rock volumes, porosity, as well as saturation, computed by integrating PNX spectroscopy and open-hole log data.

Track 1	Depth reference (measured depth), m AHORT (original rotary table)
Track 2	Zonation name
Track 3-10	Reconstruction of Titanium, Magnesium, Iron, Sulphur, Silicon, Potassium, Calcium and Aluminium dry weights with uncertainty
Track 11	Reconstruction of open hole formation resistivity (deep resistivity) with uncertainty
Track 12	Reconstruction of open hole bulk density with uncertainty
Track 13	Reconstruction of PNX TPHI with uncertainty (open hole neutron porosity was excluded from evaluation due to a poor quality)
Track 14	Cumulated rock and fluid model (colour definition is displayed in the table 9)
Track 15	Rock model
Track 16	Total porosity, inverted scale 0-0.3 v/v
Track 17	Clay corrected porosity, inverted scale 0-0.3 v/v
Track 18	Open-hole gas saturation at September 1978, scale 0-1.0 v/v
Track 19	Overlay of open-hole gas saturation and cased hole gas saturation from the recent PNX™ acquisition in April 2017, blue shading represents potential water influx in the zone below the initial GWC, scale 0-1.0 v/v
Track 20	Volume of shale, v/v
Track 21	Apparent Matrix density from open-hole MMPA compared against stand-alone PNX spectroscopy processing, g/cc
Track 22	SDR, unitless

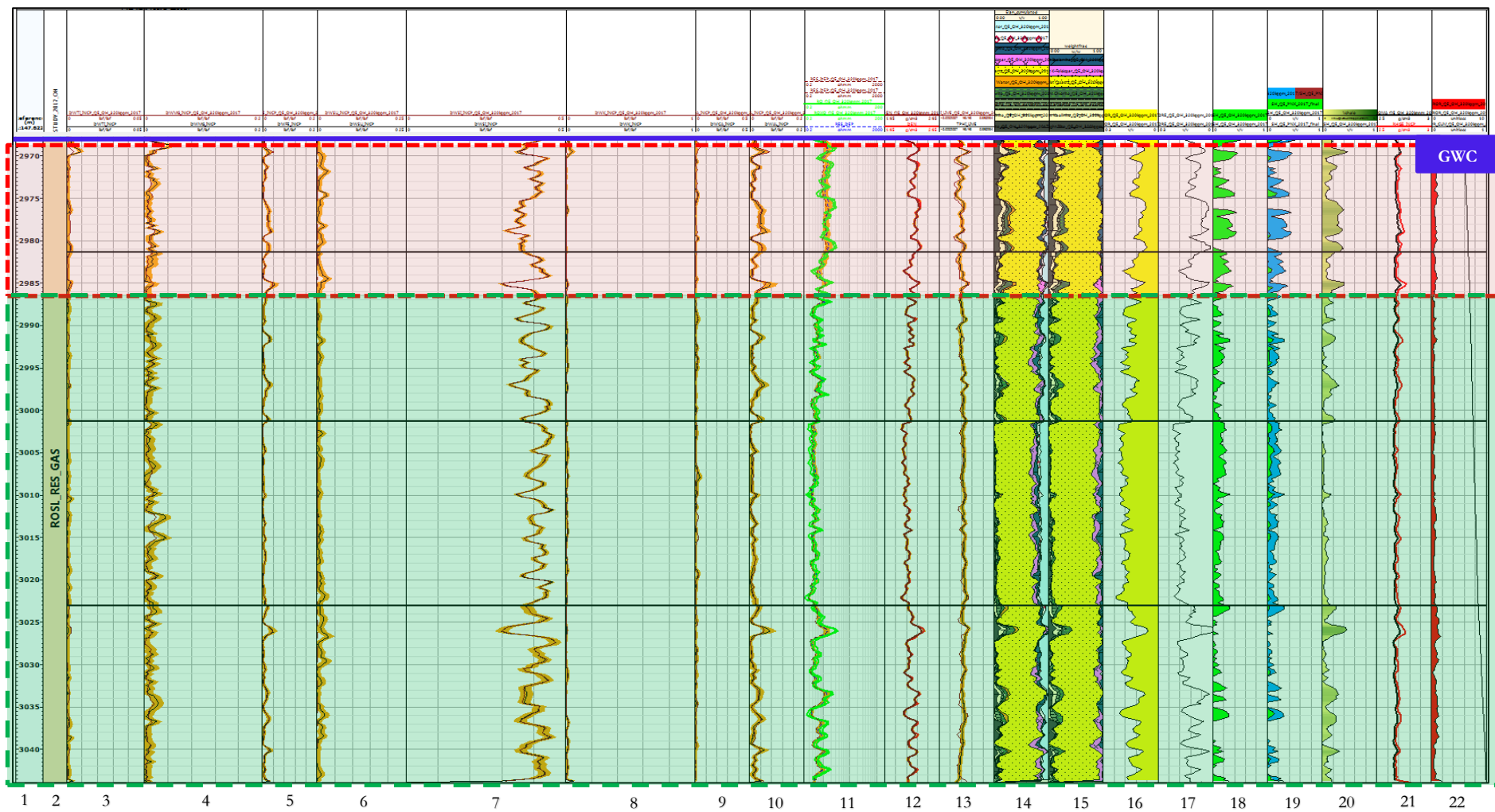


Figure 14 Cased hole MMPA main results

7.8 MMPA open hole results

A multi-mineral petrophysical analysis was performed with the open-hole data across the depth interval below the GWC. The model incorporates PNX™ spectroscopy data and available open-hole logs from 1978. It is important to note, that the resulting gas saturation is the best model estimate and does not incorporate uncertainties related to the possible ranges of gas saturation. It is revealed that the open hole saturation model for the water zone requires a more detailed study and, as a result, some changes in the saturation parameters might be expected.

The main results can be summarized as follows:

- Continuous gas saturation distribution was calculated from the initial GWC (@ 2969 m AHORT) to the well TD (@3043 m AHORT), resulting in 74 m AHORT column thickness.
- The highest gas saturation interval is observed from 2969 to 2988 m AHORT, overall 19 m of thickness. The maximum calculated gas saturation values are up to 46 % and average is around 28%.
- The interval below 2988 m AHORT is characterized by a low gas saturation with a mean equal to 14%.
- Comparative analysis of open-hole (initial saturation) and cased hole (current day) gas saturation reveals substantial difference in the interval from 2969 to 2988 m AHORT. This may indicate that the gas escaped during the production of the Groningen field. However, the mechanism of gas migration from the zone below the GWC during the depletion should be studied in more details and current observation, based on limited data, should be considered with care.

8 Generalization and delimitations

- The rock and clay mineral inputs as applied in the UHZ-1 Multi-Mineral Petrophysical Analysis for open hole and cased hole data were based on core measurements of nearby wells.
 - Slight variations in MMPA mineral concentration outputs between the open-hole and cased hole models should be expected due to different inputs logs and response equation used during modelling.
 - It is assumed that the rock composition as well as the total porosity remains unchanged during the production (depletion) history of the Groningen field.
 - Mineral concentrations based on nearby well XRD data should be used as guidance for MMPA , since it is known that the XRD measurement has possible sources of error (Herron et al.,2014), namely:
 - Core samples may be misrepresentative of log formation response because of different depth of investigation and differences in vertical resolution
 - Cores could be contaminated with mud solids or filtrate
 - Inaccurate in the analysis
 - Saturation parameters in the water leg were used congruent to the ones quoted in the 2003 petrophysical study (Van der Graaf, Seubring, 2003). That study was mainly focusing on assessment of saturation parameters for the gas zone.
-

9 Conclusions and recommendations

A petrophysical study was done to investigate the presence of gas in the aquifer of the Groningen field. The study conclusively demonstrates that there is gas below the original gas water contact at the UHZ-1 well location. The results of this study will be used for analysis in the dynamic reservoir model.

PNX™ cased hole logging technology was used to assess the gas saturation below the gas water contact in UHZ-1. Given the complexity of the topic, to assess residual gas saturation below the GWC, and sensitivity of gas saturation results to clay mineralogy, the saturation evaluation was done using a Multi-Mineral Petrophysical Analysis (MMPA).

Analysis of the cased hole PNX™ measurements suggest patchy gas saturations distribution within the first 46m below the gas water contact. The average values of around 8-10% , with peaks up to 20%. Some thin (1-2m) isolated gas filled intervals are observed deeper down, however the gas saturation values are negligible.

The 1978 open hole logs across the aquifer of UHZ-1 were also re-interpreted using MMPA Analysis (using the PNX™ spectroscopy data), applying a Waxman-Smiths saturation model. Continuous gas saturation values were interpreted along the entire logging interval within the aquifer. The maximum calculated gas saturation values are up to 46 % and average is around 28%. These saturation values are higher as compared to the cased hole analysis. However, the saturation model was derived in 2003 with a focus on the gas leg. It is recommended to re-evaluate the saturation parameters (a, m, n) with a focus specifically on the water leg. The available core data needs to be examined, and if there is sufficient data available the saturation model may potentially be further refined to incorporate details of the total clay composition within the rock.

The difference between cased hole and open hole saturation interpretation may result from various causes:

- The different methodologies for assessment of saturation both carry their own uncertainty ranges. These ranges need to be further studied.
- Impact of clay mineral composition on saturation parameter determination
 - It is known that the mineral composition has an impact on the gas saturation calculation, this is true for both open and cased hole calculations. The workflows described in this document already take this into account with the available data, however further study would be required to improve the understanding of the clay minerals and their contribution to the saturation calculation specifically below the gas-water contact. This can be achieved by a detailed calibration of PNX™ tool responses (elemental dry weights) to the core data and a detailed review of the saturation parameters used in the open-hole calculation below the gas-water contact. It is expected that this will help to reduce the difference in the interpreted saturation values between the cased hole and open hole logs.
- Impact of depletion.
 - The Open Hole logs of UHZ-1 were acquired in 1978, by which time some 650Bcm of gas was produced. As an average over the field, this equates to roughly 22% depletion with respect to initial pressure. It is possible that depletion of the aquifer has impacted the gas saturations below the gas water contact.

Once the difference is resolved, it is recommended to establish whether a representative model can be established across the full field. If so, reinterpretation of the open-hole logs for all wells with a logging coverage over the aquifer may be required. In case gas below the aquifer is observed consistently across the field, a saturation model for gas in the aquifer of the Groningen field should be constructed. To allow for extrapolation beyond the areas that have well coverage, this model build should be integrated with a geological/basin modelling explanation of the observations.

Additional points to be noted:

- Comparative analysis of open-hole (initial saturation) and cased hole (current day) gas saturation reveals substantial difference in the interval from 2969 to 2988 m AHORT. This may indicate that the gas migrated to the gas reservoir during the production of the Groningen field. However, the mechanism of gas
-

migration from the zone below the GWC during the depletion should be studied in more details and current observations, which are based on limited data, should be considered with care.

- Rock with complex mineral and clay compositions benefit from implementing of Multi-Mineral Petrophysical Analysis.
 - The Groningen field is a very sizeable field that covers quite a large geographical area. The current observations are based on PNX™ results in a single well. It is therefore advised to further investigate the presence of gas below the GWC in other areas of the field.
 - The current assessment of gas saturation below the GWC from the PNX™ and open-hole data only incorporates measurement uncertainty. No further sensitivity analysis was done due to the limited amount of available data.
 - The PNX™ spectroscopy measurements were not calibrated to core spectroscopy data of the Groningen field. It is recommended to acquire an additional PNX in a well that does have core data to allow for calibration.
-

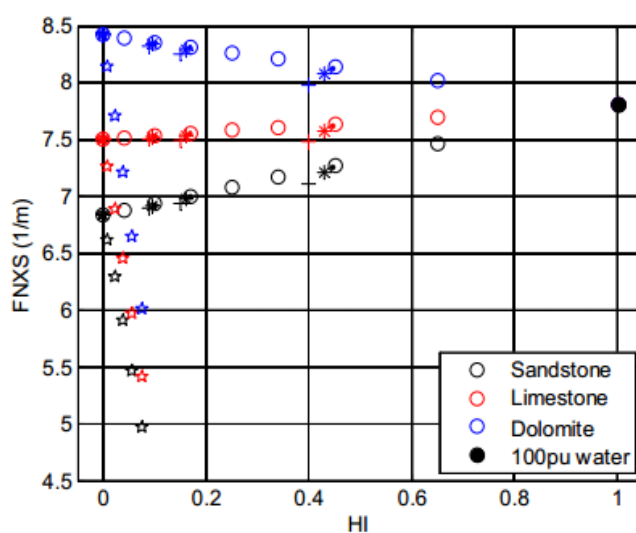
10 References

1. Van Elk, J., Study and Data Acquisition Plan Induced Seismicity in Groningen. Assen: NAM, 2016, EP201604200072.
 2. Van Oeveren, H.E.J., GFR2015: History matching and forecast uncertainty analysis. Assen: NAM,2015, EP201602208918
 3. Morris, C., Aswad, T., Morris, F. and Quinlan, T.,2005, Reservoir monitoring with pulsed neutron capture logs: Paper, SPE, Madrid, Spain,13-16 June
 4. Zhou, T., Rose, D., Quinlan, T., Thornton, Saldungaray, P., Gerges, N., Noordin, F. B. M., and Lukman, A., 2016, Fast neutron cross-section measurement physics and applications: Paper EE, *Transactions*, SPWLA 57th Annual Logging Symposium, Reykjavik, Iceland, 25–29 June.
 5. Rose, D., Zhou, T., Beekman, S., Quinlan, T., Delgadillo, M., Gonzalez, G., Fricke, S., Thornton, J., Clinton, D., Gicquel, F., Shestakova, I., Stephenson, K., Stoller, C., Philip, O., La Rotta Marin, J., Mainier, S., Perchonok, B., and Bailly, J.-P., 2015, An innovative slim pulsed neutron logging tool: Paper XXX, *Transactions*, SPWLA 56th Annual Logging Symposium, Long Beach, California, USA, 18–22 July.
 6. Rose, D., Zhou, T., Saldungaray, P., 2017, Solving for Reservoir Saturations Using Multiple Formation Property Measurements from a Single Pulsed Neutron Logging Tool: SPWLA 58th Annual Logging Symposium, Oklahoma City, Oklahoma, USA,17-21 June
 7. Visser, C., Petrographic aspects of the Rotliegend of the Groningen field. Assen: NAM, 2016, EP201609201573
 8. Rahdon, A.E., Diagenesis of the Rotliegend in Northwest Europe. Rijswijk, 1969, RKGR.0040.69
 9. Van der Graaf, A., Seubring, J., Groningen Field Review –Groningen Field Static Modelling and Ultimate Recovery Determination. Vol.4 – Reservoir Properties. Assen: NAM, 2003, NAM200308000869.
 10. JCGM 100:2008. Evaluation of measurement data – Guide to the expression of uncertainty in measurement
 11. Herron M.M., Matteson A., “Elemental Composition and Nuclear Parameters of Some Common Sedimentary Minerals,” *Nuclear Geophysics*, 1993, Vol. 7, No. 3, pp 383–406.
 12. Waxman, M.H. and Smits, L.J.M. ,1968, Electrical Conductivities is Oil-Bearing Shaly Sands, *Society of Petroleum Engineers Journal*, June.
 13. Waxman, Monroe H. and Thomas, E.C., Electrical Conductivities in Shaly Sands-I. The Relation Between Hydrocarbon Saturation and Resistivity Index; II. The Temperature Coefficient of Electrical Conductivity, 1974, *Journal of Petroleum Technology*, February
 14. Pittman, E.D., Problem related to clay minerals in reservoir sandstones. In: J.F. Mason & P.A. Dickey (Eds.), *Oil field development techniques*. AAPG Studies in Geology, 1989, 28,237-244.
 15. Kelly, S., Greenwood, J., Pattern of clay minerals diagenesis in the Rotliegend of the NE Netherlands. Assen: NAM, 1996, Rep. No. 28765.
 16. Herron, S., Herron, M., Pirie, I., Saldungaray, P., Craddock, P., Charsky, A., Polyakov, M., Shray, F., Li, T.,2014, Application and quality control of core data for the development and validation of elemental spectroscopy log interpretation: SPWLA 55th Annual Logging Symposium, Abu Dhabi, United Arab Emirates,18-22 May.
-

Appendix 1 – FNXS new measurement (courtesy of Schlumberger)

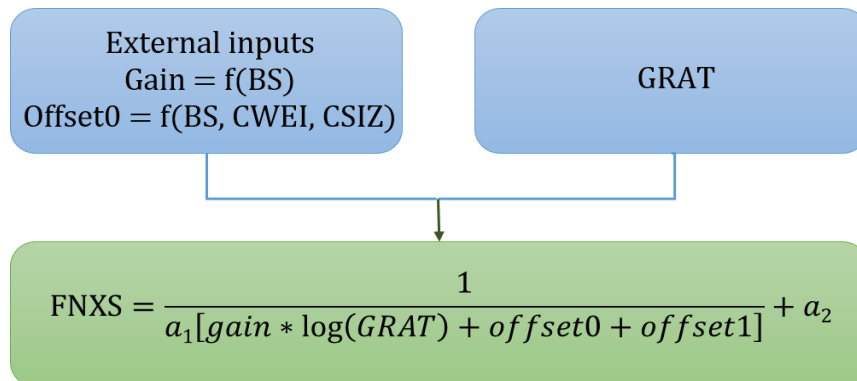
The FNXS measurement is based on fast neutrons which are indirectly measured through the detection of induced inelastic gamma rays by the logging tool. This is done using a detector (deep PNX YAP) which is coupled to the optimized source neutron pulsing scheme used by PNX. The response of the inelastic gamma ray count rate is modelled and known for a wide range of cased hole environments. There is a strong correlation between the inelastic gamma ray count rate and the 14-MeV energy elastic cross section; this is the dominant term describing the inelastic gamma ray response.

The FNXS is sensitive to the formation's atom density, which is independent from Hydrogen Index, and is therefore sensitive to the gas-filled porosity. The information is independent of other neutron measurements; hence, adding confidence and critical detail to the computed answers. In characterized interval, the FNXS also allow a standalone cased hole petrophysical analysis. In fact, FNXS is a bulk formation property which is independent of other properties and follows a linear volumetric mixing law (similar to the formation bulk density mixing law). It can be directly used for quantitative gas estimates integrated to spectroscopy, sigma, and porosity, also made available by the PNX technology. FNXS is also important to understand sigma and porosity variations in complex or unknown lithology components, because it allows to clearly distinguish between fluid and/or rock effect.



FNXS as a function of formation HI for the selected formation conditions. FNXS is not sensitive to liquid-filled porosity variations (from 0o to 100pu) or formation salinity variations (from 0 to 260ppk), but it is sensitive to gas-filled porosity variations (shown from 0 to 34pu). This confirm that FNXS is clearly an independent formation property, unrelated to HI and Sigma. Being sensitive to gas-filled porosity but insensitive to liquid-filled porosity, the measurement is important to understand the sigma data and to provide interpretation functionality similar to that of density logging, but with a different response.

The graphic below illustrates the workflow to compute FNXS from the raw measurement made by the tool (gas ratio channel, so called GRAT). Borehole corrections (corrected gain and baseline offset) based on specific well configuration are applied for log(GRAT). Additional offset (or normalization, offset 1) is applied using a no-gas filled zone for most accurate FNXS output.



Appendix 2 – Theoretical values for typical formation component (courtesy of Schlumberger)

Material	Sigma (c.u.)	TPHI	FNXS (1/m)
Quartz	4.55	-0.03	6.84
Calcite	7.08	0.00	7.51
Dolomite	4.70	0.03	8.51
Orthoclase	15.82	-0.05	6.33
Albite	7.65	-0.04	6.69
Anhydrite	12.45	-0.03	7.14
Pyrite	90.53	0.01	6.60
Bituminous Coal	15.79	0.68	7.72
Dry Illite	20.79 ^a	0.22	8.06
Wet Illite	21.00 ^a	0.34	8.02
Dry Smectite	14.36 ^a	0.29	8.36
Wet Smectite	19.23 ^a	0.68	8.60
Water	22.20	1.00	7.80
Kerogen (CH 1.3g/cm ³)	20.18	0.98	9.07
CH ₄ (0.05 g/cm ³)	2.50	-0.05	0.67
CH ₄ (0.15 g/cm ³)	7.50	0.21	2.01
CH ₄ (0.25 g/cm ³)	12.50	0.47	3.36
Oil (C ₃ H ₈ 0.5g/cm ³)	18.21	0.78	5.44
Oil (C ₃ H ₈ 0.6g/cm ³)	21.85	0.97	6.53
Diesel (CH _{1.8} 0.89 g/cm ³)	23.30	1.08	7.98
CO ₂ (0.6 g/cm ³)	0.03	-0.12	2.24

^a Field observations typically higher due to variable boron content

Appendix 3 – List of main inputs and outputs of initialization method (Techlog™ helpfile)

A3.1 Inputs

Name	Unit	Description
MFST	degC	Mud Filtrate Sample Temperature
RMF	ohm.m	Resistivity of Mud Filtrate
XWaterSalt	kppm	Flushed zone Water Salinity
RWT	degC	Formation Water Temperature
RW	ohm.m	Water Resistivity
UWaterSalt	kppm	Unflushed zone Water Salinity (formation salinity)
Mud Weight	g/cm3	Drilling Fluid Density (Mud Weight for pressure estimation)
Water Based Mud		Mud type: Water or Oil
Average Por	v/v	Average Porosity (if Porosity is not defined as an input)
Temperature	degC	Temperature at the Depth value (if Temperature is not defined as an input)
Temperature Gradient	degC/m	Geothermal gradient used to compute temperature curve (if Temperature is not defined as an input)
Depth	m	Reference depth used to compute the temperature gradient (if Temperature is not defined as an input)

A3.2 Outputs

Name	Unit	Description
SALT_XWATER	kppm	Salinity of the water in the Flushed zone
SALT_UWATER	kppm	Salinity of the water in the Unflushed zone
RHOB_IFAC	unitless	Bulk Density Invasion Factor
RHOB_XWAT	g/cm3	Water Density in Flushed zone

RHOB_UWAT	g/cm ³	Water Density in Unflushed zone
RHOB_XGAS	g/cm ³	Gas Density in Flushed zone
RHOB_UGAS	g/cm ³	Gas Density in Unflushed zone
NPHI_IFAC	unitless	Neutron Porosity Invasion Factor
NPHI_XWAT	v/v	Neutron Porosity value for the Water in Flushed zone
NPHI_UWAT	v/v	Neutron Porosity value for the Water in Unflushed zone
NPHI_XGAS	v/v	Neutron Porosity value for the Gas in Flushed zone
NPHI_UGAS	v/v	Neutron Porosity value for the Gas in Unflushed zone
NPHI_DOL	v/v	Neutron Porosity value for the Dolomite
NPHI_QUART Z	v/v	Neutron Porosity value for the Quartz
SIGMA_XWAT	v/v	Sigma value for the Water in Flushed zone
SIGMA_UWAT	v/v	Sigma value for the Water in Unflushed zone
SIGMA_XGAS	v/v	Sigma value for the Gas in Flushed zone
SIGMA_UGAS	v/v	Sigma value for the Gas in Unflushed zone
U_XWATER	b/cm ³	Volumetric Photoelectric value for the Water in Flushed zone
U_UWATER	b/cm ³	Volumetric Photoelectric value for the Water in Unflushed zone
RES_XWAT	ohm.m	Water Resistivity for the Water resistivity in Flushed zone
RES_XWAT_U NC	ohm.m	Uncertainties for the Water in Flushed zone
RES_UWAT	ohm.m	Water Resistivity for the Water in Unflushed zone
RES_UWAT_U NC	ohm.m	Uncertainties for the Water Resistivity in Unflushed zone
M_DWA	unitless	Porosity exponent in Dual Water equation
CBWA	mho/m	Apparent bound water conductivity
ALPHAQV	cm ³ /meq	QV Effective
Ftemp	degC	Formation Temperature

Addendum A

Investigation of gas presence in the
aquifer of the Groningen field

1 Introduction

This report is an addendum to the report “Investigation of gas presence in the aquifer of the Groningen field”, Reference [1]. In this addendum the results from two recent cased hole PNx acquisitions on ZRP-3A and UHM-1A are described, and the impact of these PNx results on the understanding of the presence of gas in the aquifer. Furthermore, the differences in saturation interpretation from these cased hole logs is investigated as compared to open hole logs. Lastly, the areal distribution of gas in the aquifer is investigated, based on available historical open hole data.

Note that the petrophysical evaluation of PNx data and relevant open hole data for the gas-in-aquifer study were performed with the focus on the reservoir rock below the GWC. The saturation in the gas zone was not part of the scope as this has been studied in detail in the past.

2 Additional PNx data acquisition

In Reference [1] the presence of gas in the aquifer in the Groningen field was confirmed through analysis of the UHZ-1 well. Two types of gas saturation evaluation were performed based on the available open hole and cased hole (PNx) data. In both cases the presence of gas in the aquifer was evident, however the quantities were different. It was noted that the differences in results could be due to the evaluation methodology, type of the data, a depletion effect and/or accuracy of the measurements.

To better understand the causes for differences between the cased hole and open hole saturation interpretations as well as further investigating the areal distribution of gas in the aquifer, new PNx data acquisition was performed on two additional wells. Note that only a limited number of wells in the Groningen field have significant penetration and access into the aquifer.

The ZRP-3A and UHM-1A wells were selected for PNx data acquisition because they all have a full penetration of the Rotliegend and are located relatively down-dip in the reservoir (Figure 1). Consequently, they have a long penetration of the water leg, some 175m for ZRP-3A and UHM-1A, and 100m for UHZ-1.

ZRP-3A was selected due to the following reasons:

- The most recent well with modern open hole log data (2015)
- Limited reservoir depletion (and potential depletion induced effects) between the acquisition of open hole data (2015) and PNx (2017).
- The well was drilled with Oil Based Mud, which has a limited invasion profile and effect on apparent “true formation resistivity”.

UHM-1A was selected due to the following reasons:

- The well was used to assess the areal distribution of gas in the aquifer. This is the most Eastern well where gas below the contact was observed.
 - However, the open hole log data has lower confidence because a neutron porosity log was not available.
 - PNx data acquisition was hampered by the complex completion. Thus, the results from that well were treated with lower confidence. Nevertheless, there was sufficient evidence to support the interpretation of gas presence in the aquifer.
-

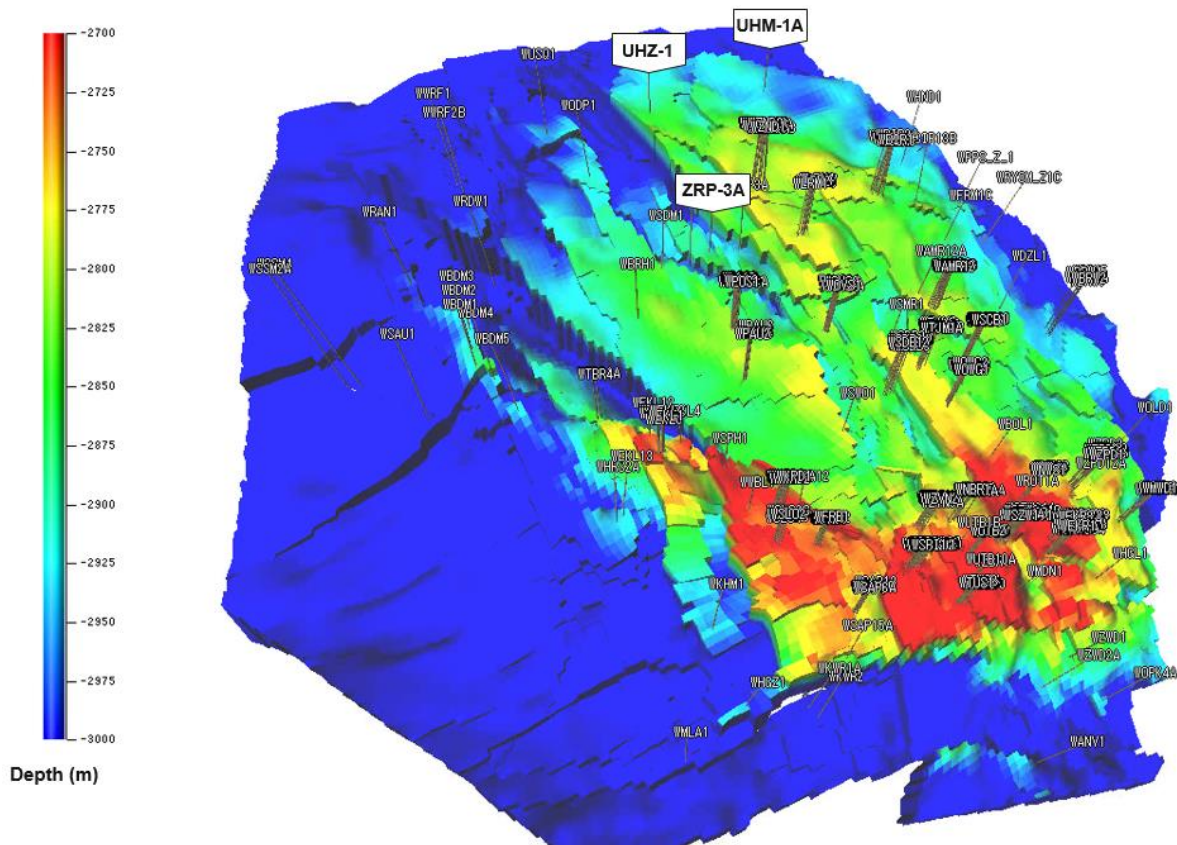


Figure 1: Depth map from the simulation grid, indicating the location of the PNx logging at wells UHZ-1, UHM-1A and ZRP-3A

3 Evaluation of PNx data

3.1 Approach

The petrophysical interpretation of PNx and open hole log data from wells ZRP-3A and UHM-1A was performed based on Multi-Mineral Petrophysical Analysis (MMPA). The approach and parameters were used as described in the previous report [1].

3.2 ZRP-3A petrophysical evaluation

On ZRP-3A the interpreted gas saturations from cased hole PNx and open hole were found to be in good agreement. Comparison analysis demonstrated that all data is in line with each other and lays within a 5-7 su uncertainty range. Thus, there is no need for revisiting the current open hole Waxman-Smiths model (OH W-S) parameters for the water leg [2].

To reach this conclusion, 4 different approaches were used to compare porosity and saturation data (for simplicity SW was used, $S_{gas} = 1 - S_w$) (see Figure 2).

- Waxman-Smiths assessment using an iterative density porosity -Waxman- Smits saturation method. (SH_WS)
- A Simple MMPA (Quanti.Elan) model using open hole Den-NEUT-RES data and simple Rock & Clay model (Quartz-Illite analogue) (SW_QE).

- PNx Quanti.Elan data using PNx cased hole data (Spectroscopy + Sigma, FNXS, TPHI), complex Rock (Quartz+K-Feldspar-Dolomite) and Clay (Illite-Kaolinite-Smectite-Chlorite) models (SW_QE_PNX_2017_final).
- Quanti.Elan model using dry volumes from PNx assessment to describe Rock & Clays and open hole DEN-NEUT-RES to describe the hydrocarbon saturation (SW_QE_OH_from_Volumes).

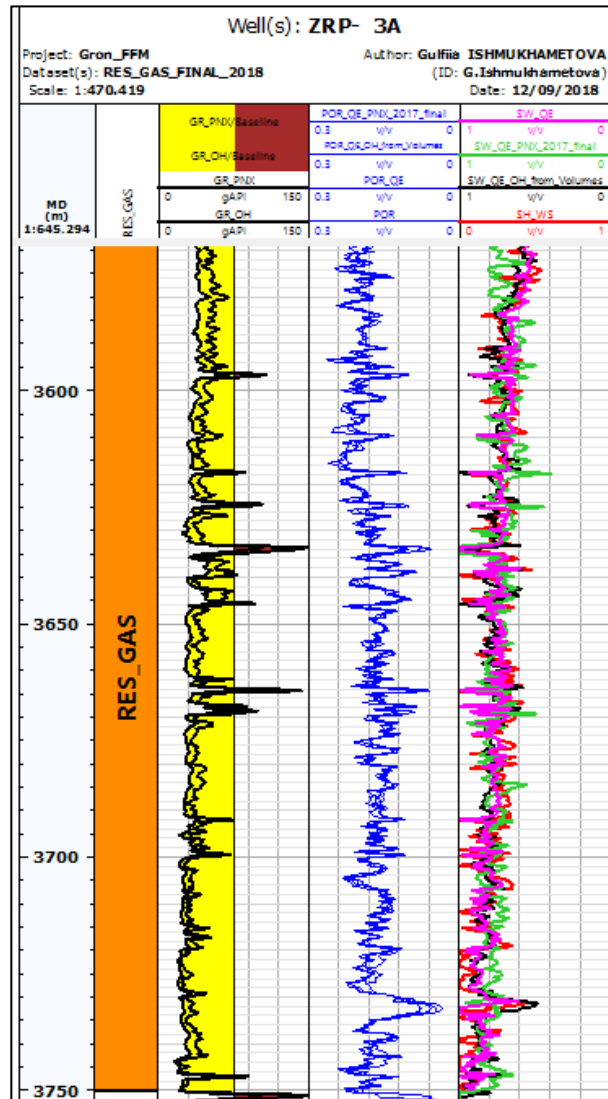


Figure 2: ZRP-3A results using 4 different approaches

3.3 UHM-1A petrophysical evaluation

UHM-1A is the oldest well on which PNx data was acquired. When the well was drilled in 1965, obviously the logging technologies were not as mature. Only a limited set of open data was recorded.

Due to limited open hole data (no neutron porosity), robustness of open hole acquisition and a complex well completion, the petrophysical evaluation was challenging for this well, both for open hole and cased hole.

Similar analysis was performed as described above for ZRP-3A. It is recommended to use results with lower confidence in comparison to ZRP-3A and UHZ-1. Both open hole and cased hole evaluations indicated the presence of gas in the aquifer. However, there is a difference between the calculated gas saturation values. The open hole evaluation indicates higher gas saturation in comparison to PNx data, the difference is around 0.1 v/v

3.4 UHZ-1 petrophysical evaluation

The interpretation was in detailed described in the previous report [1].

3.5 Comparison between ZRP-3A, UHZ-1 and UHM-1A

A comparison panel between wells ZRP-3A, UHZ-1 and UHM-1A is presented in Figure 3. The following tracks are displayed in Figure 3:

Track	ZRP-3A	UHM-1A	UHZ-1
1	Depth reference (measured depth), m AHORT (original rotary table)		
2	Zonation name		
3 -5	PNx evaluation: Full volumetric model (Illite-Kaolinite-Smectite-Chlorite-Bound Water-Quartz-K-Feldspar-Mica-Dolomite-Water-Gas), scale 0-1 v/v		
	Open hole Total Porosity, inverted scale 0-0.3 v/v		
	Open hole Gamma Ray, scale 0-150 gAPI		
6	PNx Water Saturation, inverted scale 0-1.0 v/v		
7	Open hole Water Saturation based on volumes, inverted scale 0-1.0 v/v	PNx Water Saturation based on volumes (extra sensitivity due to low confidence in data), inverted scale 0-1.0 v/v	Historical open hole gas saturation W-S, scale 0-1 v/v
8	Open hole Water Saturation using simple Quanti.Elan, inverted scale 0-1.0 v/v		
9	Gas saturation PNx vs Open hole overlay, rose- PNx > OH, grey area- PNx < OH, scale 0-1 v/v		N/A due to substantial difference
10	Difference between PNx and Open hole saturations, rose- PNx > OH, grey area- PNx < OH, scale - 1 to 1		N/A due to substantial difference

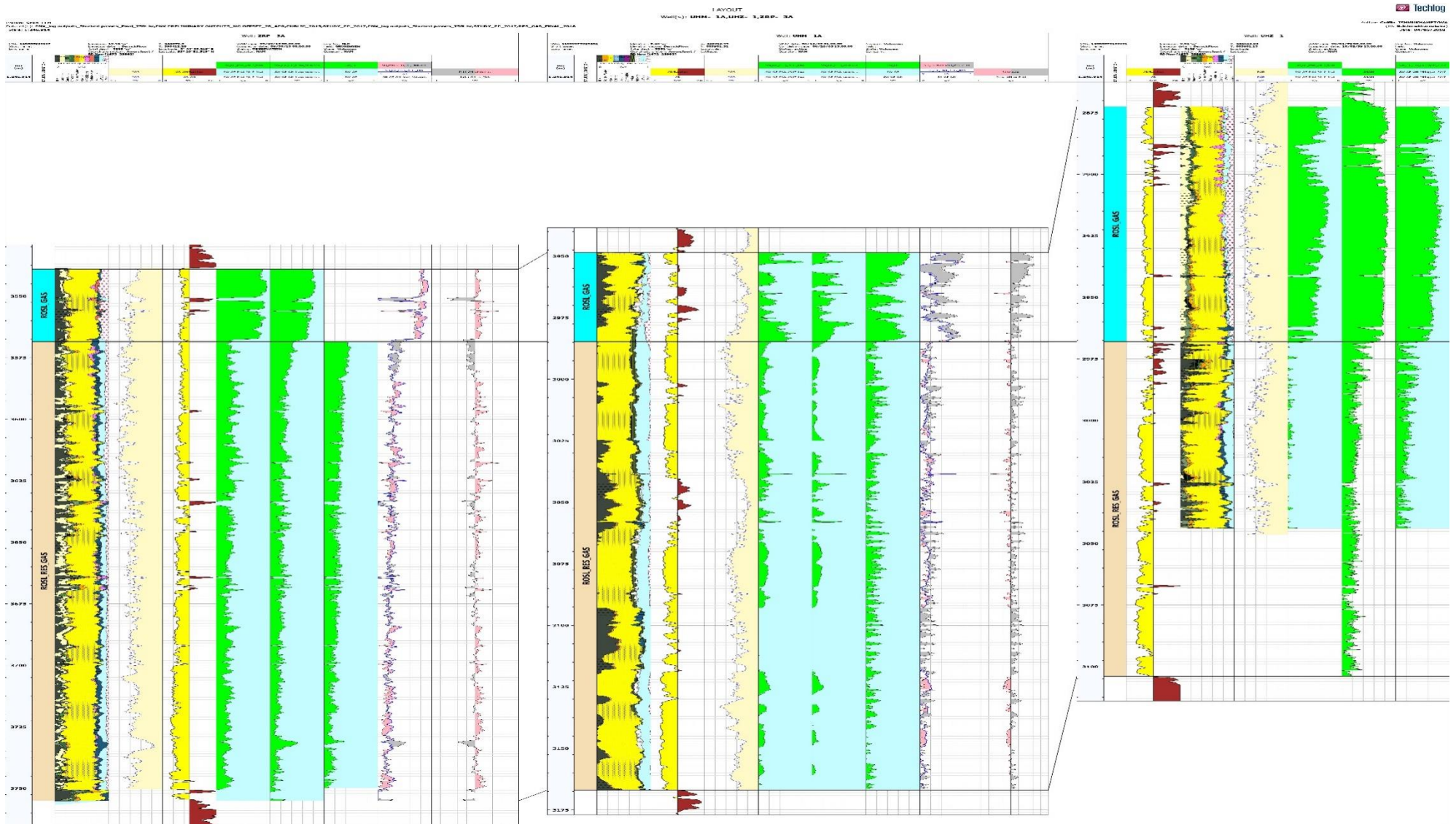


Figure 3: ZRP-3A, UHM-1A, UHZ cross section- Assessment of gas in the aquifer from different methodologies, using PNx and/or OH log data.

4 Differences between Open Hole and Cased Hole evaluation

As discussed in the Reference [1], the potential difference between OH and PNx models could be due to incorrect W-S saturation parameters, given that the main focus for the historical petrophysical work was the gas-bearing interval. However, the alignment of ZRP-3A data provided confidence in the used W-S saturation parameters for the water leg.

For wells UHZ-1 and UHM-1A more than 30 years had elapsed between the acquisition of open hole and PNx data. The combined petrophysical dataset did not allow for an assessment on the effect of depletion, nor an evaluation of saturation change over time

As confidence in the open hole saturation parameters was increased by the ZRP-3A data, other potential reasons for misalignment between OH and CH evaluations were studied. Both the effect of resistive mud invasion on resistivity readings and type of resistivity measurement were selected for further investigation.

5 Evaluation of Open Hole data

5.1 Types of resistivity measurements

A number of different approaches can be used to calculate water saturation, based on different saturation calculation models, like Archie or Waxman-Smits, as well as with various types of input resistivity logs. The most commonly used two types of resistivity logs are induction and laterlog based resistivity methods. There are a lot of literature available that in details describes the benefits of using one vs another. The focus in this study was on type of log resistivity in the context of “apparent true formation resistivity” in high formation water salinity, as Groningen formation water is known to be highly saline (salinity around 260 kppm).

Laterlog resistivity is a well-established technology and the majority of all wells in Groningen were logged with it. The main requirement is that such data can only be acquired in a water-based mud environment due to the measurement physics. This is quite a shallow measurement, certainly with the older tool types and is better suited to describe near wellbore environment and less the “true formation resistivity” (resistivity of zone with no effect of mud infiltration, virgin formation).

Induction resistivity is a more recent technology and is amongst other things dependent on the type of measurement (phase shift resistivity, attenuation resistivity), measurement frequency & transmitter-receiver distances. This measurement can read deep into the formation and is estimated to be a better approximation for the value of “true formation resistivity”. The induction log can be run in both an oil-based mud as well as a water-based mud environment. The modern tools, which are available in the market in addition to raw logs also supply inversion resistivities. This helps to better estimate the “true resistivity” (see Figure 4, [Ref 3]).

Most of the available Groningen induction log data falls under the category of single/dual induction with the effect of shoulder beds (The Rotliegend is a laminated formation). The advanced resistivity inversion methodologies are not applicable. Thus, the assumption was made, that the deepest induction log represents the apparent “true formation resistivity”.

The problem arises, that the majority of Groningen wells were drilled with water-based mud with salinities much lower than the formation water (see Table 1). For evaluation of gas zone saturation this will not significantly skew the results, however for the water leg, where the quantities of gas are small, minor variations on the resistivity measurement due to resistive fluid invasion effects can result in an erroneous “gas in the aquifer” calculation.

Imaging Invasion with Resistivity Logs			
Logging Technique	Invasion Analysis	Requirements	Advances
Present Capabilities			
Single induction	Assume $R_t = \text{ILD}$	Shallow invasion	—
Dual induction	Tornado chart correction	Bed thickness > 8 ft [2.4 meters]; no shoulder bed effect; $R_{xo} > R_t$ (monotonic)	Corrects for invasion when requirements are met
Dual induction (R & X signals) with multilevel deconvolution	Tornado chart correction	Beds > 4 ft [1.2 meters]; $R_{xo} > R_t$ (monotonic)	Deeper depth of investigation; useable and reliable tornado chart software; includes correction for shoulder-bed effects; thin-bed corrections in many cases
Dual laterolog with R_{xo}	Tornado chart correction	Beds > 4 ft; $R_{xo} < R_t$ (monotonic)	Handles $R_{xo} < R_t$
Simple, multiple depth of investigation induction (multifrequency or simple arrays)	Tornado chart correction	Same as dual induction	R & X signals
	Apparent resistivity profiles	Gradual changes in radial resistivity; beds > 4 ft; direct measurement of R_{xo} and R_t	May detect nonmonotonic resistivity profiles; limited resistivity range
Future Improvements			
Advanced inductions that are both multifrequency and multiaray	Constrained inversion	Gradual vertical changes in invasion profile; beds > 4 ft; R_{xo} not much less than R_t	Resistivity profile extrapolated to R_{xo} and R_t ; high-resolution answers free of borehole effects
Combination of advanced induction and dual laterolog with R_{xo}	Constrained inversion	Gradual vertical changes in invasion profile; beds > 4 ft	Induction images conductive regions; laterolog images resistive regions
Combination of logging while drilling (LWD) and wireline resistivities	Constrained inversion	High-quality LWD data	Handles arbitrarily deep and complex invasion at wireline time

Figure 4: Invasion analysis overview [Ref 3]

5.2 Invasion Profiles

To further portrait the “true formation resistivity” topic, it is important to understand what the mud invasion is and what the zones of investigation are. The invasion topic was brought to attention in the 1950’s and since then there are still no direct measurement available in the market to definitively answer the question: “What is the true formation resistivity?”.

Deep invasion of water-based mud (WBM) filtrate affects all resistivity logs, and, in the extreme, the available resistivity log may be used only qualitatively. At the opposite extreme, when oil-based mud (OBM) filtrate invades a hydrocarbon reservoir, the invading OBM filtrate generally displaces only the reservoir oil and gas, leaving the S_w unchanged. Here, invasion of OBM usually does not change the deep-formation or the invaded-zone resistivity in the water leg.

To emphasize, the assessment of “true formation water resistivity” for Groningen field is quite complex task and more in-depth study might be required. This could entail integration with laboratories, core analysis and new water sample analysis and still may lead to no definitive results. Within the scope of this study all differences are attributed to type of the resistivity log run.

The open hole resistivity measurements are affected by the invasion of water-based mud. The water zone is more sensitive to changes in resistivity in comparison to the gas leg, due to high formation water (260 kppm). It is nearly impossible to accurately correct the measured resistivities for the changed resistivity due to the drilling mud invasion, this especially holds for older data from 1970-1990.

Most of the wells were drilled with water-based mud, with salinities varying from 30 up to 200 kppm (see Table 1).

	Well	QELAN Model	YEAR	MUD	Mud Salinity (kppm)	FW salinity (kppm)	RES IND	Zones	Flag Name	Top	Bottom	Gross	Av_Porosity
1	BDM- 1	YES	1977	WBM	122	260	NO	RES_GAS	RES_GAS	3171.6	3255.4	83.8	0.115
2	BDM- 4	YES	2008	OBM	260	260	YES	RES_GAS	RES_GAS	3402.5	3500.2	97.6	0.154
3	BIR- 13B	YES	1989	WBM	69	260	YES	RES_GAS	RES_GAS	3992.7	4052.4	59.7	0.183
4	KHM- 1	YES	1989	WBM	106	260	NO	RES_GAS	RES_GAS	3954.0	4034.0	80.0	0.123
5	ODP- 1	YES	1977	WBM	249	260	NO	RES_GAS	RES_GAS	3095.7	3269.7	174.0	0.161
6	PPS-Z 1	YES	1989	WBM	64	260	YES	RES_GAS	RES_GAS	3280.3	3430.8	150.6	0.153
7	RYSM- Z1C	YES	1989	WBM	31	260	YES	RES_GAS	RES_GAS	3893.2	4059.7	166.4	0.183
8	SAU- 1	YES	1995	WBM	207	260	NO	RES_GAS	RES_GAS	3467.5	3741.9	274.4	0.185
9	UHZ- 1	YES	1978	WBM	130	260	NO	RES_GAS	RES_GAS	2985.0	3103.7	118.6	0.166
10	ZRP- 2	YES	2014	OBM	260	260	YES	RES_GAS	RES_GAS	3221.2	3411.4	190.2	0.159
11	ZRP- 3A	YES	2015	OBM	260	260	YES	RES_GAS	RES_GAS	3568.5	3749.9	181.4	0.175

Table 1: Overview of wells used for resistivity sensitivity

Figure 5 is a schematic illustration of depth of investigation versus invaded zone. It is not the aim of this report to explain this in detail as it is well documented in literature.

It should be noted that two types of invasion are available (in relation to the water leg):

- Resistive invasion occurs when the mud filtrate resistivity is higher than the formation water resistivity. To translate this into salinity, when the mud filtrate salinity is lower than the formation water salinity (Groningen example).
- Conductive invasion occurs when mud filtrate resistivity is less than the formation water one.

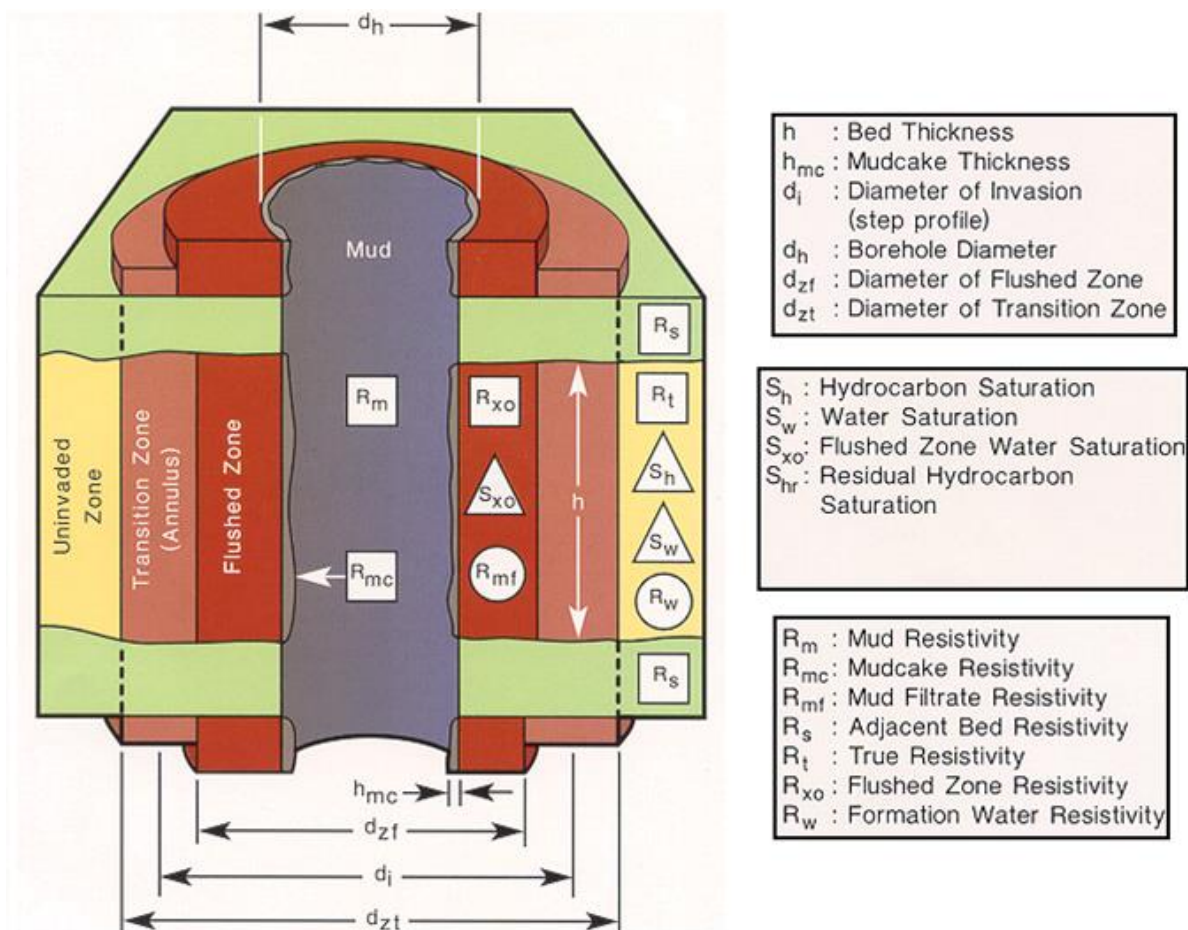


Figure 5: Schematic illustration of depth of investigation versus invaded zone [Ref.4]

5.3 Saturation assessment: Induction resistivity vs Laterlog

To get a better handle on the effect of invasion of gas in the aquifer saturation assessment, the differences between Induction (IND) and Laterlog (LL) derived saturations were investigated. The induction log has a larger depth of investigation than the laterlog. Hence the LL is more sensitive to mud invasion.

The database was reviewed for all wells with both laterlog and induction log coverage over the reservoir. Only a limited number of wells have both IND and LL resistivity measurements: BIR-13 B, RYSM-Z1C, PPS-Z1 (see table 1,2). The rest of the wells suitable for MMPA evaluation have only LL data.

	Well	Zones	Flag Name	Top	Bottom	Gross	Av_Por	IND LOG	COMMENTS
1	BDM- 1	RES_GAS	RES_GAS	3171.6	3255.4	83.8	0.115	NO	all data
2	BDM- 2	RES_GAS	RES_GAS	3146.3	3170.8	24.5	0.183	NO	limited res gas column
3	BDM- 4	RES_GAS	RES_GAS	3402.5	3500.2	97.6	0.154	YES	all data
4	BDM- 5	RES_GAS	RES_GAS	4920.4	4950.7	30.4	0.164	NO	limited res gas column
5	BIR- 2A	RES_GAS	RES_GAS	3060.4	3104.3	43.8	0.159	NO	no neutron porosity, not a full dataset
6	BIR- 3	RES_GAS	RES_GAS	2991.4	3023.0	31.5	0.176	NO	no neutron porosity, not a full dataset
7	BIR- 6	RES_GAS	RES_GAS	2993.3	3032.6	39.3	0.158	NO	no neutron porosity, not a full dataset
8	BIR- 13B	RES_GAS	RES_GAS	3992.7	4052.4	59.7	0.183	YES	all data
9	BRH- 1	RES_GAS	RES_GAS	2993.4	3050.9	57.5	0.146	NO	no neutron porosity, dataset was not full
10	HGZ- 1	RES_GAS	RES_GAS	3679.5	3695.3	15.9	0.051	YES	Very low porosities, saturation can be affected by tight rock.
11	LRM- 7	RES_GAS	RES_GAS	2981.7	2994.5	12.8	0.102	NO	limited res gas column
12	ODP- 1	RES_GAS	RES_GAS	3095.7	3269.7	174.0	0.161	NO	all data
13	PAU- 2	RES_GAS	RES_GAS	2992.0	3013.4	21.4	0.159	YES	limited res gas zone
14	PAU- 3	RES_GAS	RES_GAS	2994.7	3010.7	16.0	0.158	YES	limited res gas zone
15	POS- 4	RES_GAS	RES_GAS	2987.5	3002.0	14.5	0.130	NO	limited res gas column
16	POS- 9	RES_GAS	RES_GAS	2994.4	3000.6	6.2	0.136	NO	limited res gas column
17	PPS- Z1	RES_GAS	RES_GAS	3280.3	3430.8	150.6	0.153	YES	all data
18	RDW- 1	RES_GAS	RES_GAS	3175.8	3355.1	179.3	0.142	NO	data-quality issue, washouts, res strange
19	RYSM- Z1C	RES_GAS	RES_GAS	3893.2	4059.7	166.4	0.183	YES	only res gas zone
20	SDM- 1	RES_GAS	RES_GAS	3014.8	3070.4	55.6	0.181	YES	no neutron porosity, not a full dataset
21	TBR- 4	RES_GAS	RES_GAS	3012.8	3037.9	25.1	0.145	NO	limited res gas column
22	UHM- 1A	RES_GAS	RES_GAS	2984.7	3166.2	181.5	0.128	NO	the dataset is not full, no neutron porosity, will not be used
23	UHZ- 1	RES_GAS	RES_GAS	2985.0	3103.7	118.6	0.166	NO	
24	USQ- 1	RES_GAS	RES_GAS	2986.5	3209.4	222.9	0.160	NO	TWO SATURATION AVAILABLE, THE LOWEST WAS SELECTED, NO NEUTRON POROSITY
25	WRF- 1	RES_GAS	RES_GAS	3134.0	3370.7	236.8	0.170	NO	TWO SATURATION AVAILABLE, THE HIGHEST WAS SELECTED, mostly res gas zone
26	WRF- 2B	RES_GAS	RES_GAS	3972.7	4004.1	31.4	0.206	NO	TWO SATURATION AVAILABLE, THE HIGHEST WAS SELECTED, limited res gas zone
27	ZRP- 1	RES_GAS	RES_GAS	2994.2	3102.9	108.7	0.148	NO	no neutron porosity, not a full dataset
28	ZRP- 2	RES_GAS	RES_GAS	3221.2	3411.4	190.2	0.159	YES	full dataset

29	ZRP- 3A	RES_GAS	RES_GAS	3568.5	3749.9	181.4	0.175	YES	full dataset
30	ANV-3							NO	low porosities, tight rock, res can be compromised
31	HRS- 2A							NO	limited res gas zone
32	KHM- 1							NO	full dataset
33	MOW-Z-1							NO	different formation responses, not a best analogue
34	OPK-2A							NO	different from overall wells log response, not recommended for stage 1 study, not a classical example
35	OPK-3A							NO	different from overall wells log response, not recommended for stage 1 study, not a classical example
41	SAU- 1							NO	only res gas zone, full dataset
42	SDB- 1							NO	limited res gas zone
43	ZND-11B							NO	limited res gas zone
44	ZND- 1							NO	limited res gas zone
45	ZND- 9A							NO	limited res gas zone
46	ZWD-2A							NO	limited OH data

Table 2: Review of available well penetrations in the aquifer (depths in meters MD)

MMPA analysis was performed for both RYSM-Z1C and PPS-Z1 and using both IND & LL as a separate scenario.

Figure 6 compares interpreted gas saturations from both the induction log and laterlog for wells Paapsand-Z1 and Rysum-Z1C. These wells were drilled with Water-Based-Mud (salinities of 64 and 31 kppm, respectively).

It is evident, that Sgr (gas in the aquifer saturation) from IND resulted in lower Sgr values in comparison to LL keeping everything else the same. For PPS-Z1 the difference is up to 10 su with an average of 6 su, for RSM-Z1 the difference is up to 18 su, with an average of 10 su.

In accordance to this, the assessment of Sgr LL for the wells, drilled with the water-based mud salinity < 260 kppm, will always resulted in higher Sgr IND for Groningen field. This is due to the following reasons:

- Due to resistive mud invasion
- Shallow depth of investigation of Laterlog readings on comparison to Induction log.
- Difference in the physics of the measurements between LL and IND.

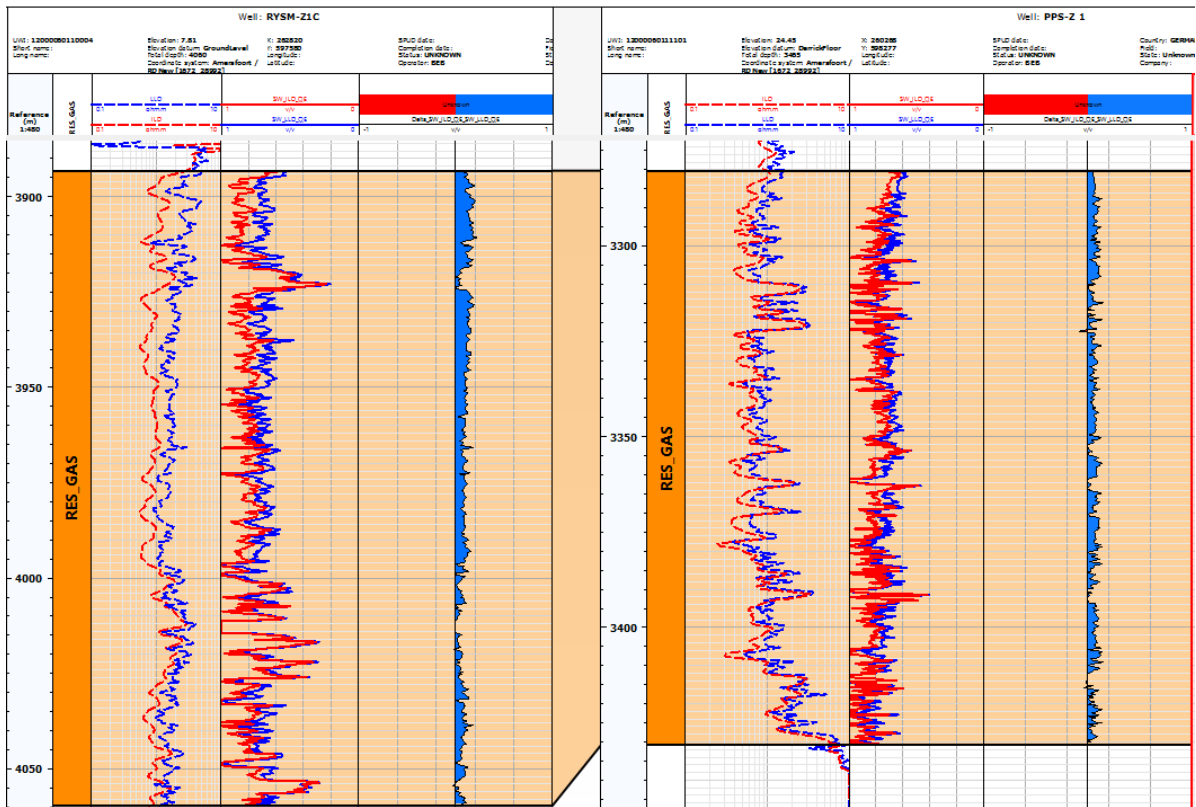


Figure 6: Comparison of interpreted saturations from LL versus IND for wells RYSM-Z1C and PPS-Z1. (Track 1- depth reference, *m*AHORT, Track2- Zonation, Track3-Resistivity overlay, IND in red, LL in blue, scale 0.1-10 Ohm-m, Track4- Water saturation (*S_w*) overlay IND vs LL, inverted scale 0-1 v/v, Track5- Delta in *S_w*, scale - 1 to 1, blue area *S_{gr}* LL>*S_{gr}* IND)

5.4 Uncertainties based on ZRP-3A

After comparison of the data open hole and cased hole PNx data it is evident that ZRP-3A is the well with the highest confidence data in comparison to UHZ-1 and UHM-1A well, for both open-hole and cased hole data, which demonstrate good alignment.

The uncertainty analysis of saturation calculations for open hole and cased hole evaluation was performed on the basis of ZRP-3A

The uncertainty analysis was done using Monte-Carlo simulations both for open hole W-S and PNx MMPA evaluations with 1000 cycles.

The selected uncertainties for PNx and W-S open hole evaluation are listed in the Figure 7 & 8. The uncertainty of each selected measurement for PNx is statistical uncertainty from processing the raw data (*_SIG*). see table 3. W-S uncertainties were taken from historical report[Ref. 2].

Uncertainties			
	Uncertainties	Uncertainty Type	Activate
Shallow temperature	0.05	Relative	no
Shallow Qv	0.05	Relative	no
Wet Clay Porosity	0.05	Relative	no
CEC	0.05	Relative	no
Rsh	0.05	Relative	no
CBW	0.05	Relative	no
Neutron Porosity	0.05	Relative	no
UI_Aluminum Weight Fraction	DWAL_SIG_INCP	Absolute	yes
UI_Calcium Weight Fraction	DWCA_SIG_INCP	Absolute	yes
UI_Potassium Weight Fraction	DWK_SIG_INCP	Absolute	yes
UI_Silicon Weight Fraction	DWSI_SIG_INCP	Absolute	yes
UI_Sulfur Weight Fraction	DWSU_SIG_INCP	Absolute	yes
UI_Iron Weight Fraction	DWFE_SIG_INCP	Absolute	yes
UI_Magnesium Weight Fraction	DWMG_SIG_INCP	Absolute	yes
UI_FNXS	FNXS_SIG	Absolute	yes
Neutron Porosity constants	TPHI_SIG	Absolute	yes
UI_Aluminum Weight Fraction constants	0.05	Relative	no
UI_Calcium Weight Fraction constants	0.05	Relative	no
UI_Potassium Weight Fraction constants	0.05	Relative	no
UI_Silicon Weight Fraction constants	0.05	Relative	no
UI_Sulfur Weight Fraction constants	0.05	Relative	no
UI_Iron Weight Fraction constants	0.05	Relative	no
UI_Magnesium Weight Fraction constants	0.05	Relative	no
UI_FNXS constants	0.05	Relative	no
Bulk Density	0.027	Absolute	no
Bulk Density constants	0.05	Relative	no
UI_Titanium Weight Fraction	0.05	Relative	no
UI_Titanium Weight Fraction constants	0.05	Relative	no
UI_Sigma Formation	SIGM_SIG	Absolute	yes
UI_Sigma Formation constants	0.05	Relative	no
Porosity	0.05	Relative	no
Porosity constants	0.05	Relative	no

Figure 7: PNx uncertainties selection for ZRP-3A

	<u>Uncertainties</u>		
	Uncertainties	Uncertainty Type	Activate
Deep a	0.05	Relative	no
Deep m	0.05	Absolute	yes
Deep n	0.1	Absolute	yes
Formation Water Resistivity	0.001	Absolute	yes
Deep Temperature	0.05	Relative	no
Deep Qv	0.05	Relative	no
Shallow a	0.05	Relative	no
Shallow m	0.05	Relative	no
Shallow n	0.05	Relative	no
Mud Filtrate Resistivity	0.05	Relative	no
Shallow Temperature	0.05	Relative	no
Shallow Qv	0.05	Relative	no
Wet Clay Porosity	0.05	Relative	no
CEC	0.05	Relative	no
Rsh	0.05	Relative	no
CBW	0.05	Relative	no
Bulk Density	0.027	Absolute	yes
Neutron Porosity	0.05	Relative	no
Formation Resistivity	0.05	Absolute	yes
Flushed Zone Resistivity	0.05	Relative	no
UI_Gamma Ray	0.05	Relative	no
Bulk Density constants	0.05	Relative	no
Neutron Porosity constants	0.05	Relative	no
UI_Gamma Ray constants	0.05	Relative	no

Figure 8: Waxman-Smiths open-hole uncertainties for ZRP-3A

DWAL_SIG_I NCP (lbf/lbf)	DWCA_SIG_IN CP (lbf/lbf)	DWK_SIG_INCP (lbf/lbf)	DWSI_SIG_IN CP (lbf/lbf)	DWSU_SIG _INCP (lbf/lbf)	DWMG_SI G_INCP (lbf/lbf)	FNXS_SIG (1/m)	TPHI_SIG (ft3/ft3)	SIGM_SIG (cu)
0.009	0.005	0.003	0.022	0.003	0.004	0.011	0	0.053

Table 4: ZRP-3A PNx measurement uncertainties for the curves highlighted in the Figure 7.

Based on above, the average 1STD values to assess uncertainty (2STD) of gas saturation in the Aquifer in the Groningen field (see Figure 9, 10).

- W-S OH- 1 STD- 0.05 v/v (based on uncertainty of the W-S input parameters)
- PNx CH- 1 STD- 0.034 v/v (statistical uncertainty around PNx measurements, not accounting for any mineralogical differences)

To conclude for ideal logging environment, like in ZRP-3A (clean vertical well, single completion with small diameter) the assessment of gas saturation from cased hole PNx is equivalent to open hole evaluation. However, this statement will hold ONLY for ZRP-3A data. Other cases should be evaluated separately.

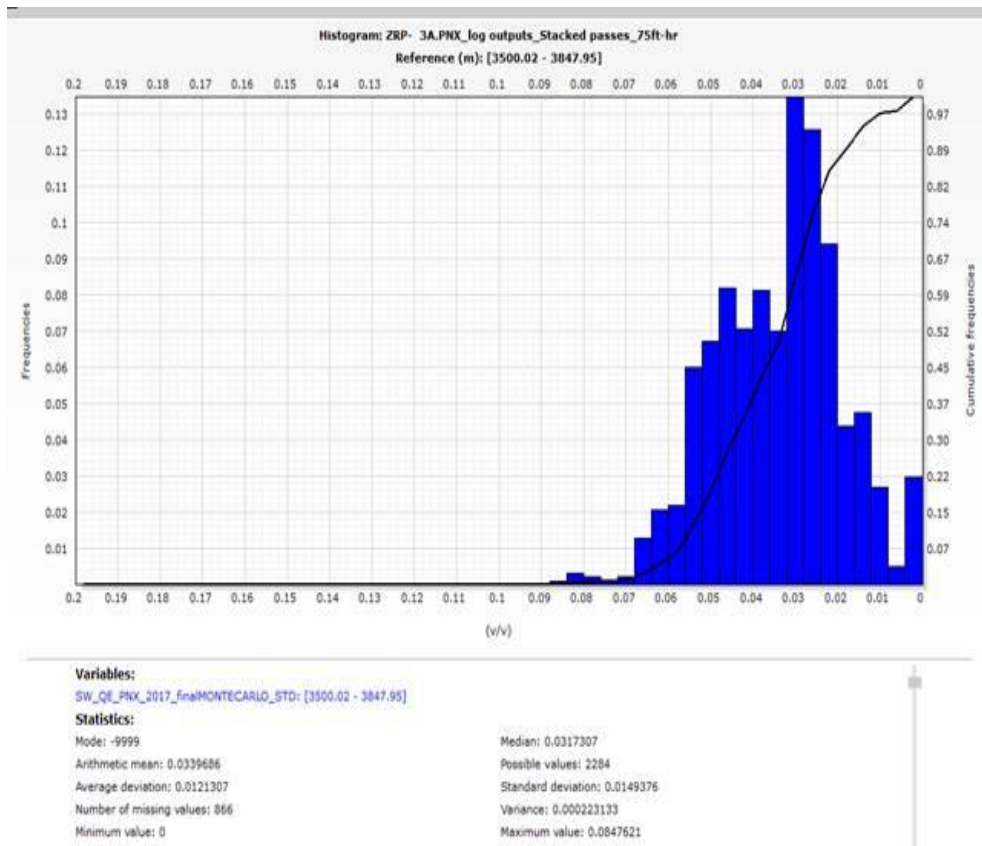


Figure 9: Uncertainty analysis on the ZRP-3A PNX cased hole, Monte-Carlo, 1 STD distribution

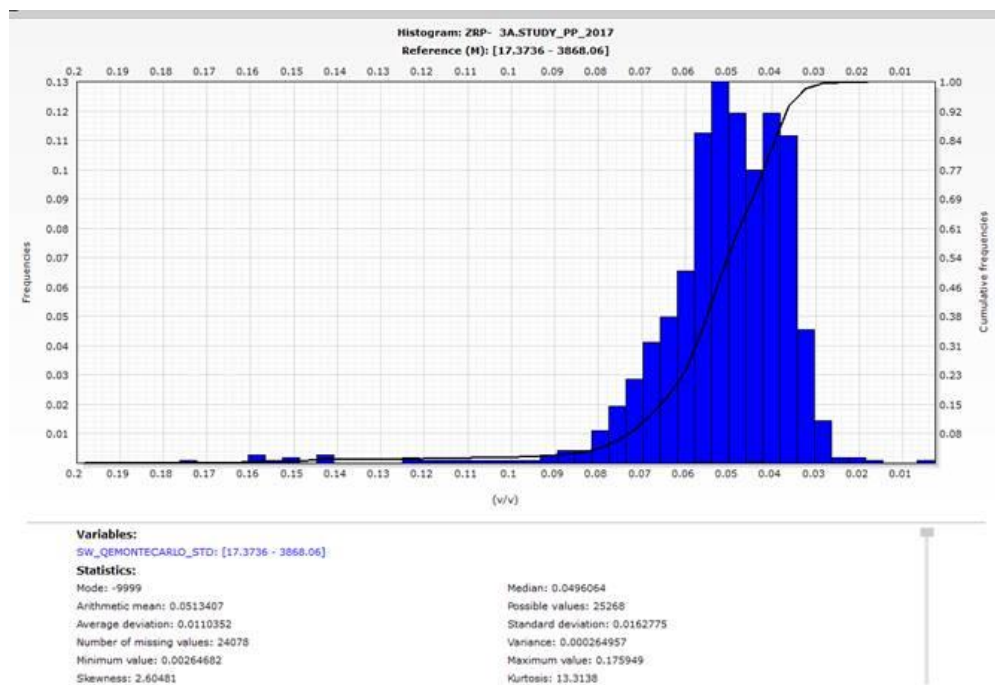


Figure 10: Uncertainty analysis on the ZRP-3A, W-S model, Monte-Carlo, 1 STD distribution

6 Gas in the Aquifer Ranges

The ranges for gas in the Aquifer for the Groningen field are based on the ZRP-3A data and uncertainty analysis.

The Sgr for gas in the aquifer range is based on the ZRP-3A:

- ZRP-3A PNx results
 - Sgr MEAN = 0.26 v/v
 - Sgr MIN&MAX – Sgr MEAN +/- 2STD PNx CH
- ZRP-3A Open Hole (OH W-S) results
 - Sgr MEAN = 0.23 v/v
 - Sgr MIN&MAX – Sgr MEAN +/- 2STD OH WS
- The average 1STD values to assess Sgr measurement uncertainty (2 STD) are as follows:
 - W-S OH- 1 STD- 0.05 v/v
 - PNx CH- 1 STD- 0.034 v/v

7 Conclusions

- Interpretation of gas leg unchanged
 - The 2012 interpretation of gas saturations above the contact was not changed as part of this study.
- Existing OH Waxman-Smits model is valid in water leg.
- Induction resistivity is the recommended for the open hole Sgr evaluation.
- Gas-in-aquifer saturation interpretation is very sensitive
 - To interpret saturations of gas-in-aquifer, complex petrophysical models need to be used (Multi-Mineral Petrophysical Analysis). These models require a large suite of input parameters, which complicates the search for unique solutions and contributes to the uncertainty ranges of the results.
- Mismatch of saturation estimate between OH and PNx below the contact for UHZ-1 can be explained by the uncertainty in the OH interpretation as well as the PNx interpretation.
- The ranges for gas in the aquifer should be based on the ZRP-3A data.

8 Recommendations

- There is an opportunity to correlate PNx spectroscopy data to core measurement at ZRP-3A.
 - PNL analysis of the historical data to assess saturation profiles.
 - Investigate impact of mineralogical model and uncertainties of PNx measurement on saturation parameter determination on UHZ-1.
-

9 References

- [1] G. Ishmukhametova, "Investigation of gas presence in the aquifer of the Groningen field, EP201707201356", NAM, Assen, 2017
 - [2] Van der Graaf, A., Seubring, J., "Groningen Field Review –Groningen Field Static Modelling and Ultimate Recovery Determination. Vol.4 – Reservoir Properties, NAM200308000869". NAM, Assen 2003.
 - [3] D. Allen et. al, "Invasion", Schlumberger, Oilfield Review magazine, July 1991.
 - [4] H. Liu, "Principles and application of well logging, Electrical logging", Springer Mineralogy, 2017
-

